scientific reports

OPEN

Investigating the failure mechanisms of cascade landslide dams under overtopping conditions: an experimental approach

Changjing Fu[1,2,4✉], Tianlong Zhao[1,3✉], Hongxin Li[1] & Di Huo[1]

Under strong earthquakes and extreme rainfall conditions, landslide clusters near rivers may block incoming water flows, forming cascade landslide dams. When subjected to extreme hydrological conditions, these cascade landslide dams can experience overtopping, which erodes and entrains material from the dam surface, compromising dam stability, which can potentially lead to outburst flooding. Although existing research provides valuable insights into landslide dam failures, it falls short in addressing the complexities of cascading failures in dam groups. The influence of various factors on this intricate process is still only partially understood, highlighting the need for a comprehensive understanding of dam surface evolution and flood flow dynamics specifically within the context of cascading failures in landslide dams. In this study, we conduct physical model experiments to categorize the stages of cascade landslide dam failure, identify typical failure modes, and investigate the mechanisms affecting breach morphology evolution and flood flow development during cascading failures. Our findings reveal that cascade landslide dams can amplify floods during cascading breaches, with peak flow rates increasing progressively from upstream to downstream. In cascade systems, downstream dams experience accelerated breach processes, where layer erosion becomes predominant. Significant fluctuations in river water levels between cascades can lead to slope failures in both upstream and downstream dams. Specifically, downstream dams exhibit more rapid breach widening, fewer instances of collapse at the breach slope compared to upstream dams, and earlier peak flow timing, making cascade landslide dam breaches more challenging for emergency response. These observations highlight the notable differences between cascade landslide dam failures and single dam failures. Based on these findings, we provide insights into developing mathematical models for cascade landslide dam failures to improve physical-based flood predictions, which will assist the development of early warning strategies for cascade landslide dam breach floods.

Keywords Cascade landslide dams, Dam break experiment, Cascade failure mechanism, Breaching characteristics

During intense seismic events and extreme rainfall, multiple large-scale landslides may occur along a river channel from upstream to downstream. In narrow mountainous valleys, these large-scale landslides can potentially block the river channel, forming cascade landslide dams[1–3]. For instance, the May 12, 2008, Wenchuan earthquake triggered over 100 landslide dams[4–6]. Many rivers experienced dense clustering of landslides and debris flows, exhibiting a bead-like distribution along the river channels in the earthquake-affected region[7]. For example, in the Tongkou River, nine cascade landslide dams formed within a 30 km stretch; in the Mianyuan River, four landslide dams formed along the river from upstream to downstream; in the Shiting River, one landslide dam formed on average every 0.88 km within an 8 km range; in the upper reaches of the Anzi River, four landslide

[1]Key Laboratory for Hydraulic and Waterway Engineering of Ministry of Education, Chongqing Jiaotong University, Chongqing 400074, People's Republic of China. [2]Department of Civil Engineering, Monash University, Clayton, VIC 3168, Australia. [3]Department of Infrastructure Engineering, University of Melbourne, Parkville, VIC 3010, Australia. [4]National Key Laboratory of Water Disaster Prevention, Nanjing Hydraulic Research Institute, Jiangsu, China. ✉email: nhri_fuchangjing@163.com; ztl1986@163.com

dams were distributed over a 7.5 km stretch; and in the Qing River, three landslide dams were distributed within a 5 km stretch[8,9]. Notably, in the Gengda to Yingxiu river section spanning 33 km, 25 landslide dams were created by the earthquake[3,10,11], as shown in Fig. 1. Different from conventional artificial dams, natural landslide dams typically comprise unconsolidated and poorly sorted materials and are vulnerable to failure following flow overtopping[1]. According to statistical analysis[12–14], over 80% of these landslide dams breach within one year. If a cascading failure of landslide dams occurs, it will lead to more severe flash floods than the failure of a single landslide dam[15–17], causing severe damage to human lives and property downstream.

The failure mechanism of a single dam due to flow overtopping, along with the resulting hydraulic and morphological impacts, has been studied both experimentally[18–24] and numerically[1,25–28]. Previous research on single landslide dam failures has mainly focused on the geomorphological evolution of the landslide dams and downstream river channels, as well as the hydrodynamic process. For instance, Zhou[29] investigated the effects of upstream inflow on the timescales and magnitudes of peak discharges and the time to the inflection point through physical flume experiments. This study also examined the mechanisms influencing the non-uniform morphological evolution of landslide dam breaches, specifically the non-linear variation of the dam surface gradient[30]. Additionally, field experiments on dam collapses caused by the combined influence of seepage flows and overtopping water were conducted by Zhou[22] to evaluate the contribution of seepage flows to the overtopping failure of landslide dams, focusing on dam stability, breach duration, and flow discharge. Zhou[31] conducted a series of laboratory experiments to investigate the effects of granular material composition, sliding width, and valley shape on the deposition morphology of landslide dams, revealing the significant influence of these factors on dam height, length, and cross-valley profiles. To verify the applicability of widely used erosion equations for the erosion rates, Zhu[32] conducted 12 sets of model experiments, revealing discrepancies between measured and calculated erosion rates and suggesting the need for future improvements in these empirical models. A recent large-scale field experiment by Zhang[33] conducted in a natural river channel reveals the connection between hydrodynamic processes and the geomorphic effects of breach floods. Additionally, Muslim[34] and Mahmood[35] developed advanced image enhancement techniques to improve the clarity and accuracy of experimental observations, which can significantly benefit the visualization and analysis of data in similar experimental studies.

The aforementioned findings provide important insights into landslide dam failure research. However, they cannot be directly applied to the cascading failure of landslide dam groups. This is because the chain reaction in landslide dam clusters not only demonstrates greater destructive power but, more importantly, reveals more complex failure mechanisms. To elucidate these mechanisms, some investigations[17,36–38] have been conducted to explore the cascading failure of landslide dams. It is known that dam breach is a physical process involving the transfer of flow-energy. For cascade landslide dams, the transfer of energy during failure can be obstructed, diminished, or amplified by downstream dams, depending on various factors such as the size of the dams, the spatial arrangement between them, and the hydrodynamic conditions at the time of failure. These factors
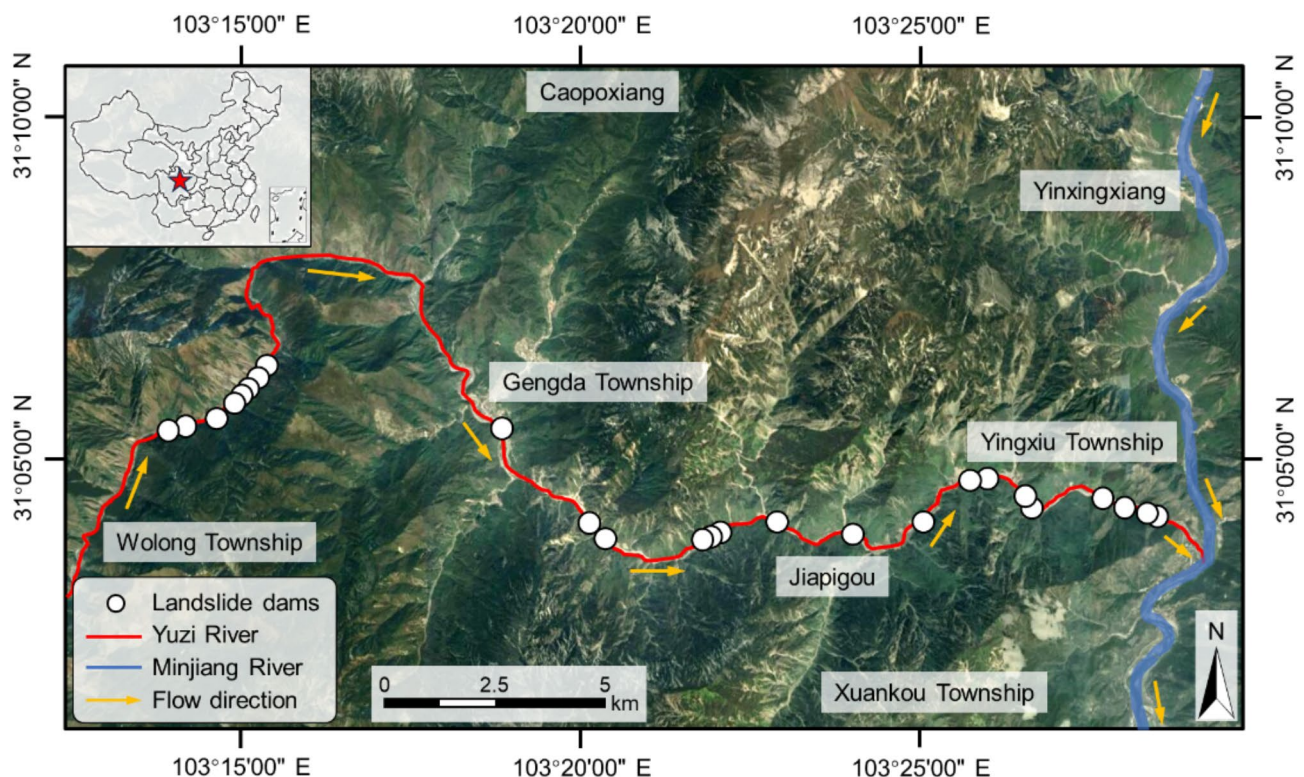
Fig. 1. The distribution of landslide dams in the Gengda to Yingxiu section of the Yuzi River.

significantly influence the breach dynamics by providing abundant sediment materials for subsequent processes, yet current research has not clarified how these factors interact and shape the cascading failure process. Furthermore, the mechanisms underlying overtopping failures in cascaded landslide dams remain insufficiently explored.

To bridge these research gaps, this study systematically investigates the cascading failure process of cascade landslide dams through U-shaped flume experiments ("Methodology" section). It focuses on analyzing the geomorphological evolution of dam surfaces, hydrodynamics, and the progression of flood waves between the steps ("Experimental results" section). Moreover, the study explores the influencing factors and underlying patterns of cascading dam failures, compares these mechanisms with those of single dam failures, and highlights their distinct features ("Discussion" section). Finally, the limitations of this study and directions for future research are discussed in detail ("Conclusions" section), providing a framework to advance understanding of this complex and underexplored phenomenon.

Methodology
Test equipment
In practical scenarios, landslide dams are often distributed along winding and meandering river valleys[39]. Some landslide dams may form at river bends, such as the Tangjiashan landslide dam[40], while others may be located in straight sections of the river, such as the Baige landslide dam[41]. Cascade landslide dams are particularly prone to such varied distributions. To reasonably simulate the deposition locations of landslide dams and the resulting flow dynamics induced by these locations, the authors selected a U-shaped flume to replicate the cascading failure process of landslide dams in this study.

The experiments to investigate the mechanisms of overtopping failure in cascade landslide dams were conducted using a high-precision U-shape test system. The device has an overall accuracy of ±0.5 mm and consists of three parts: a water supply system, a U-shape, and a tailwater collection pool. For the water supply system, the flow rate can be controlled by setting the flow rate on the industrial computer to supply water as needed for the experiment. The supply and return water control system, based on frequency conversion technology, can generate continuous non-uniform flow processes of any shape. The U-shape consists of three parts: a straight channel section, a curved channel section, and another straight channel section. The sidewalls are made of tempered glass for observing the dam breach process and water flow conditions within the flume. The internal effective dimensions are 26.5 m in length, 0.4 m in width, and 0.4 m in height. The tailwater collection pool is located underground to capture the experimental tailwater and any sediment transported by the flow. Given that the slope of most natural riverbeds ranges from 0° to 3°, the slope of the experimental flume was set at 0.057°, corresponding to a slope ratio of 1/1000. Three model dams were placed along the flume, as shown in Fig. 2.

Model design
Understanding the dimensional and shape parameters of landslide dams is crucial for accurately simulating their behavior, especially in the context of cascading failures. Peng[13] and Zhou[29] conducted statistical analyses on the dimensions of 80 real-world landslide dams. Building on this, Shi[42] analyzed the relationships between these dimensions and determined the typical ranges for these parameters, as shown in Table 1. To enhance the accuracy of simulating cascading failures, this study determined the dimensions of the three model dams (Dam 1, Dam 2, and Dam 3) used in the experiments based on these previously established parameters. The specific values for the model dams are summarized in Table 1. Comparing the morphological parameters of the model dams with the statistical ranges of 80 real-world landslide dams, it is evident that all model parameters fall within the range of the case library.

Considering the effective internal height of the experimental flume, which is 40 cm, and ensuring that the three model dams can sequentially undergo overtopping failure, the heights of the three model dams were determined to be 24 cm, 22 cm, and 20 cm, respectively. Additionally, all three model dams were set to have the same crest width of 20 cm. Based on the morphological parameter relationships outlined in Table 1, the specific dimensions of the model dams were established. The detailed values are presented in Table 2. The axis length of the three model dams is the same as the internal width of the flume, measuring 40 cm. To ensure that the water flow does not overflow the entire cross-section of the dam during overtopping failure and to observe the development of the breach in different dimensions, initial spillway channels were excavated on the sides of the dam crests of the three model dams before the experiment. The cross-sections of these spillway channels are triangular, with a top width of 10 cm and a depth of 6 cm, as illustrated in Fig. 1.

Dam materials
Based on the material composition of landslide dams, Liang[43] classified them into three categories: soil, mixed, and rockfill. This study focuses on the most common type, mixed-type landslide dams, to determine the material composition for the model dams. To ensure that the materials used in the model accurately represent real-world conditions, data from Shan[44] were utilized. This dataset includes the material composition of 86 landslide dams worldwide. Specifically, the particle size composition of 54 mixed-type landslide dams was statistically analyzed, resulting in the particle size distribution shown in Fig. 3a. The characteristic particle size parameters derived from this analysis are summarized in Table 3.

From Fig. 3a, it is evident that the characteristic particle sizes of real-world mixed type landslide dams exhibit numerous outliers, which are predominantly skewed towards the larger size range, resulting in a right-skewed distribution. In this context, the mean is not a representative measure; thus, the median is used as the basis for calculating the gradation of the model dams. Due to the size constraints of the flume, the gradation needed to be scaled down using a mass substitution method. The maximum particle size was set to 1/10 of the flume's internal width, corresponding to 40 mm. Particles exceeding this size limit were proportionally replaced with finer
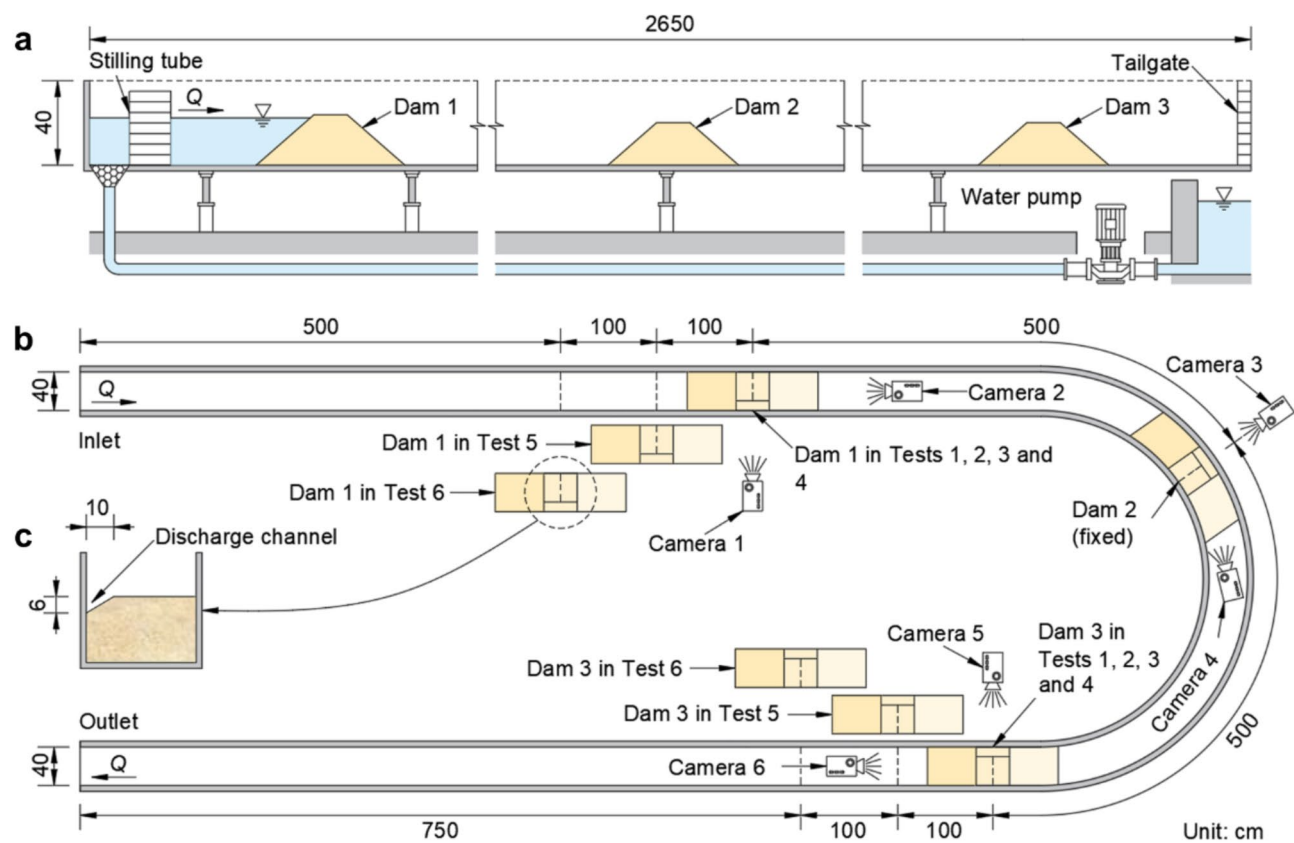
Fig. 2. Schematic diagram of the experimental setup: (**a**) Elevation view (expanded); (**b**) Plan view; (**c**) Downstream elevation view.

Dam ID	H/C	H/B	S_u (°)	S_d (°)	$V_d^{1/3}$/H	$V_l^{1/3}$/H	L:H
Real-world dams (Shi et al.[42])	0.20–3.00	0.02–1.00	11.00–45.00	11.00–45.00	0.50–5.00	0.20–10.00	17.60–222.00
Dam 1	1.20	0.29	36.87	36.87	1.53	2.77–3.17	20.83–35.00
Dam 2	1.10	0.28	36.87	36.87	1.60	3.37–3.69	
	1.00	0.27			1.67	3.61–3.94	
Dam 3	1.00	0.27	36.87	36.87	1.67	3.61–3.94	

Table 1. Morphological characteristic parameters of landslide dams. In the table, H is the dam height, C is the crest width, B is the dam bottom width, S_u is the upstream slope angle, S_d is the downstream slope angle, $V_d^{1/3}/H$ is the dam shape coefficient, $V_l^{1/3}/H$ is the barrier lake form coefficient, and L/H is the step spacing coefficient.

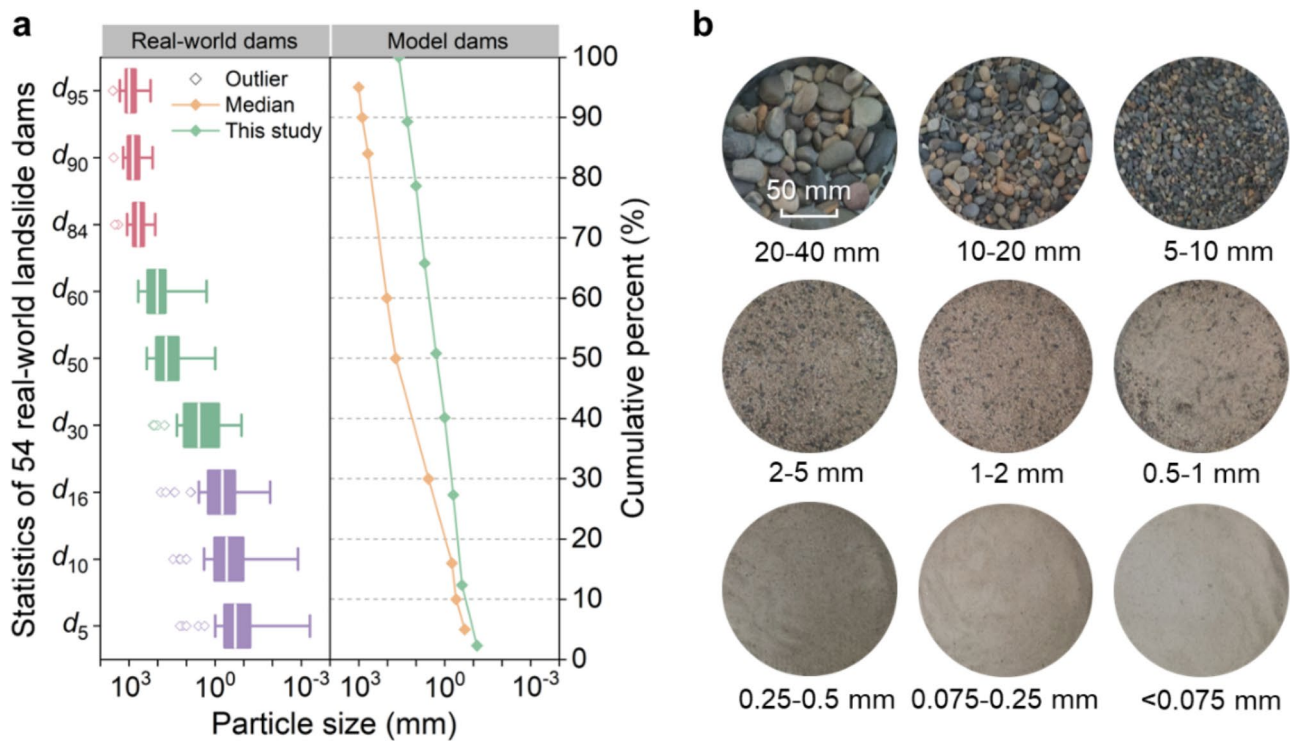| Section design parameter	Dam 1	Dam 2		Dam 3
Crest width (cm)	20	20		20
Width of dam bottom (cm)	84	78.67	73.33	73.33
Dam height (cm)	24	22	20	20
Slope of upstream dam (°)	36.87	36.87		36.87
Slope of downstream dam (°)	36.87	36.87		36.87

Table 2. Dimensions of model dams.

Fig. 3. Materials for the model dams: (**a**) Particle size distribution; (**b**) Sieved particle groups.

Statistics	Particle size (mm)								
	d_5	d_{10}	d_{16}	d_{30}	d_{50}	d_{60}	d_{84}	d_{90}	d_{95}
Maximum	1	2.4	3.7	21.5	240	478	1150	1607.1	2105
Q_3	0.47	1.05	1.775	12	112	225	725	1096	1300
Q_1	0.06	0.105	0.2075	0.74	19	54	308	445	592
Minimum	0.005	0.0013	0.012	0.12	1	2	122	151	178
Median	0.2	0.4	0.56	3.7	51	104	475	749	995
Mean	1.1	2.2	5.5	17.6	83.8	159.0	633.6	887.9	1138.2

Table 3. Characteristic particle size statistics of 54 real-world mixed-type landslide dams. In the table, Q_3 represents the upper quartile in statistics, and Q_1 represents the lower quartile.

particles based on their relative content. This approach ensured that the gradation curve of the model materials remained consistent with that of the prototype. Using the adjusted gradation curve, the content of each particle group was calculated, enabling material sieving and preparation for the experiments, as illustrated in Fig. 3b.

Measurements

The experiments conducted in this study focus on investigating the effects of upstream inflow, middle dam height, and step distance between cascade dams on the dam breach process. The categories A, B, and C in Table 4 correspond to these three variables, respectively. Since this experiment did not aim to rigorously simulate a specific real-world landslide dam, the inflow rates were not scaled based on prototype landslide dam data. To avoid scenarios where the inflow rate was either too low to mobilize dam particles or too high, leading to an instantaneous and complete dam breach that would hinder observation, a series of preliminary tests were conducted to determine appropriate inflow rates for the experiment. Ultimately, the inflow rates were set at 7.84 L/s, 9.37 L/s, and 9.84 L/s. To establish the step distances between the model dams, the concept of the step distance coefficient was introduced, defined as the ratio of the average step distance of landslide dams along a river to the dam height. Based on an analysis of 34 cascade landslide dam cases reported by Chen[45], it was observed that the step distance coefficient for real-world cascade landslide dams ranged from approximately 17.60 to 222.00 (Table 1). Accordingly, the step distances for this experiment were determined to be 500 cm, 600 cm, and 700 cm. In this study, a total of six experiments were conducted, and the specific test conditions are detailed in Table 4.

According to the experimental setup, the model dams were constructed, followed by the installation of cameras and measuring scales, which were used to monitor geomorphological changes during the tests. The

Category	Test ID	Upstream inflow (L/s)	Height of Dam 2 (cm)	Step distance (cm)
A	1	7.84	22	500
	2	9.37	22	500
	3	9.84	22	500
B	1	7.84	22	500
	4	7.84	20	500
C	1	7.84	22	500
	5	7.84	22	600
	6	7.84	22	700

Table 4. Summary of test conditions.
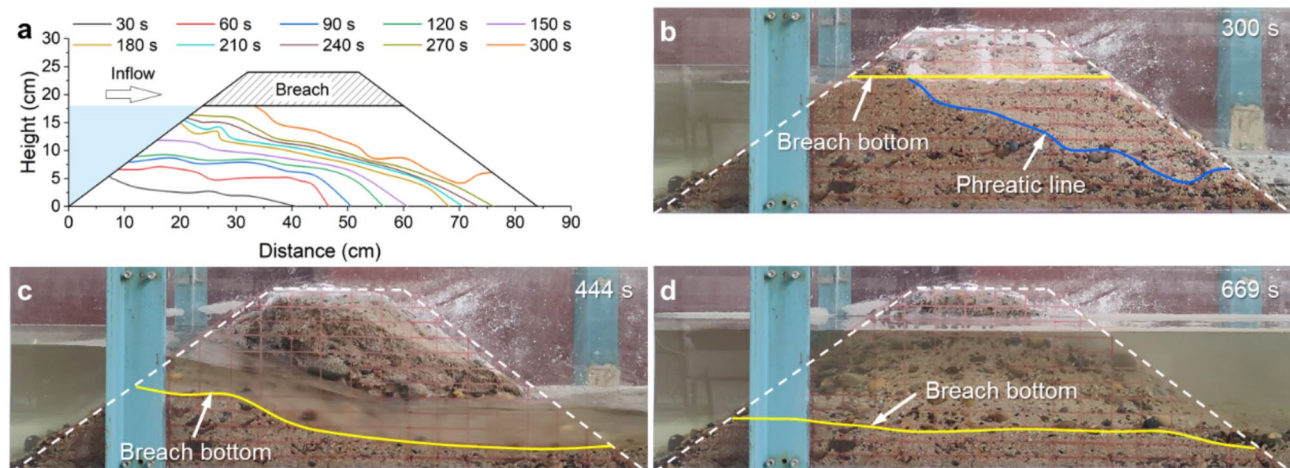
Fig. 4. Typical features in failure process (Dam 1 in Test 1): (**a**) Evolution of the phreatic line; (**b**) Phreatic line; (**c**) Overtopping breach; (**d**) Submersion of the residual dam. $t=0$ indicates the beginning of the impoundment.

experiments were then initiated by adjusting the flume's water supply system, and the entire dam breach process was meticulously recorded using the cameras.

Experimental results
General features

The results indicate a general similarity in the cascade failure process of landslide dams across the six test groups. Overall, the progressive failure of each landslide dam involves three typical stages: rise of the phreatic line, overtopping breach, and submersion of the residual dam. The main characteristics are as follows: After the landslide dam forms, the upstream water level rises continuously due to inflow, causing the phreatic line within the dam to also rise, as illustrated in Fig. 4a. The inclination of the phreatic line is related to the permeability of the dam - the lower the permeability, the steeper the inclination, and this inclination is independent of the downstream slope of the dam. When the upstream water level rises to the base of the breach, as shown in Fig. 4b, overtopping occurs. The overtopping flow removes soil and rock particles from the breach and downstream dam slope, causing deformation and further erosion, initiating the breach process, similar to the overflow failure described by Zhao[46], as shown in Fig. 4c. As the reservoir water continues to flow out, the water head difference between the upstream and downstream levels decreases, reducing the flow velocity. When the flow can no longer mobilize the dam particles, the breach process ceases. However, due to the water-blocking effect of the downstream dam, the water level rises, submerging the residual dam in the reservoir formed by the downstream dam, as shown in Fig. 4d. For the last dam in the river channel, since there is no downstream dam to block the water, the submersion process does not occur, and the breach outflow level gradually decreases to zero in the end.

Breaching mode

By analyzing the video data from the breaching experiments of cascade landslide dams, it has been found that different levels of landslide dams exhibit both similarities and differences in the longitudinal and transverse development speed of the breach, development patterns, breach flow rates, and upstream and downstream water levels throughout the breaching process. Based on these breach development and water flow change patterns, the breaching processes of Dam 1 and Dam 2 can be broadly divided into five stages, while Dam 3 can be divided into four stages. Here, we select a typical test group, Test 1, as an example to analyze the changes in water flow

and morphology during the breaching process of cascade landslide dams. The images of the breaching process are shown in Fig. 5. For the sake of facilitating comparative analysis among the three dams, Dam 2 was mirrored without affecting the study's conclusions.

The division of the breaching stages and the breach development patterns for each cascade landslide dam are as follows:

Stage I: Diversion erosion. In this stage, the reservoir water level rises and gradually exceeds the bottom of the discharge channel. Overflow water begins to pass through the discharge channel and flow downstream. However, the flow velocity at the breach is usually low at this stage, and only a small portion of fine particles on the breach surface can be carried away by the overflow water. Consequently, irregular scour pits start to appear on the surface of the downstream slope, and the breach development is primarily characterized by vertical incision. Additionally, at the upstream entrance of the dam crest, due to the water flow converging towards one side of the discharge channel, part of the upstream slope soil is carried into the discharge channel, forming a funnel-shaped entrance. This causes the water surface width upstream of the discharge channel to be greater than that of the downstream slope. For Dam 2 and Dam 3, this stage is mainly influenced by the scouring effect of breach waves generated by the upstream dam failure, and the scouring process is not continuous.

Stage II: Headward erosion. As the breach continues to deepen, the water head at the breach increases, resulting in higher flow velocity and intensified erosion. The irregular downstream slope formed in the previous stage is further scoured into multiple levels of scour pits, and the breach exhibits headcut erosion. In this form of erosion, the soil on the leeward side of the headcut is eroded while deposition occurs on the windward side. Consequently, the slope of the leeward side of the headcut is typically less steep than that of the windward side. Measurements show that the slope angle of the leeward side ranges from 22° to 39°, while the windward side ranges from 9° to 24°. Due to the different erosion forms on the windward and leeward sides of the scour pits, soil particles move downstream, but the scour pits geometrically migrate upstream, exhibiting headward erosion. Additionally, the breach bottom width rapidly expands during this stage, leading to small-scale collapses on the breach side slopes, which is the primary mode of breach top width expansion.

Stage III: Breach development. During this stage, the flow rate at the breach gradually reaches its peak, and the erosion intensity is at its highest. Soil particles of all sizes can be mobilized, and the bottom of the breach starts to become more uniform. The depth and bottom width of the breach primarily expand continuously, while the top width of the breach mainly increases suddenly due to collapses. These collapses involve not only the side slopes of the breach but also the upstream and downstream slopes of the dam.

Stage IV: Backflow inundation. Due to the obstruction caused by the downstream landslide dam, the breach wave progressing downstream generates backflow when it reaches the downstream landslide dam. This causes the downstream water level to rise continuously, leading to the inundation of the upstream dam. During this process, the breach wave propagates between the two adjacent downstream landslide dams, resulting in intermittent small-scale collapses on the upstream slope of the downstream dam. Figure 6a illustrates the manner in which the downstream dam's slope collapses during this stage. For the upstream dam, the breaching process has already ended by this stage, and the dam body is fully saturated, leading to fewer collapses. It is worth noting that in this experiment, since Dam 3 does not have a downstream dam, there is no backflow inundation.

Stage V: Water level decrease. Due to the breaching of the downstream dam, the reservoir water level begins to drop continuously, causing the upstream dam, which was previously submerged, to gradually become exposed. During this stage, the continuous decrease in water level may lead to collapses on the downstream slope of the upstream dam, resulting in further enlargement of the breach. The primary reason for this is the difference in permeability between the inside and outside of the dam body, leading to outward-directed seepage within the dam. The downstream slope of the dam may collapse under the influence of seepage forces. Figure 6b illustrates the collapse of the upstream dam's downstream slope caused by the lowering water level during this stage. The breaching process ends when the water level drops to a point where the flow through the breach is insufficient to mobilize any soil particles.

It is important to note that the breaching mode revealed in this experiment, where slope collapses on both upstream and downstream dams are caused by the breaching wave and water level fluctuations in the river channel, is not universally applicable. Summarizing the breaching processes and flow parameters of dams under all test conditions, the breaching patterns and flow parameters of cascade landslide dams are presented in Table 5. The occurrence of this breaching mode is influenced by numerous factors, such as the characteristics of the breaching wave from the upstream dam, the geological and structural properties of the downstream dam slope, the hydraulic conditions of the downstream dam body, as well as the channel and topographical features of the river. These factors introduce significant complexities to the study of cascade dam breaching. Accurate flood modeling for cascade dam breaches requires considering a broader range of influencing factors, which poses substantial challenges to the development of mathematical models for cascade dam breaching.

After analyzing the evolution of cascade dam breaches in all test conditions, this study identifies two dominant breaching patterns: headcut erosion and layer erosion. These patterns are defined based on the longitudinal development characteristics of the breach. Specifically, the formation of scour pits and the accompanying headcut erosion phenomenon in breaches can be attributed to the complex mechanisms initiated by the heterogeneity of dam slope soil at the micro level. This is a significant difference compared to naturally formed sand waves in riverbeds. This mechanism primarily involves the cohesive properties of the soil and its wide-graded structure, both of which contribute to the heterogeneous initiation of the soil.

Regarding soil cohesion, its heterogeneity leads to an uneven distribution of bonding forces between clay particles, resulting in significant differences in the conditions required to initiate different particles (such as flow velocity and shear force), ultimately causing heterogeneous initiation of the soil. For wide-graded soils, the significant particle size differences between large and small particles directly lead to notable differences in initiation flow velocity. In the early stages of dam breaching, when the breach flow is still relatively low, these
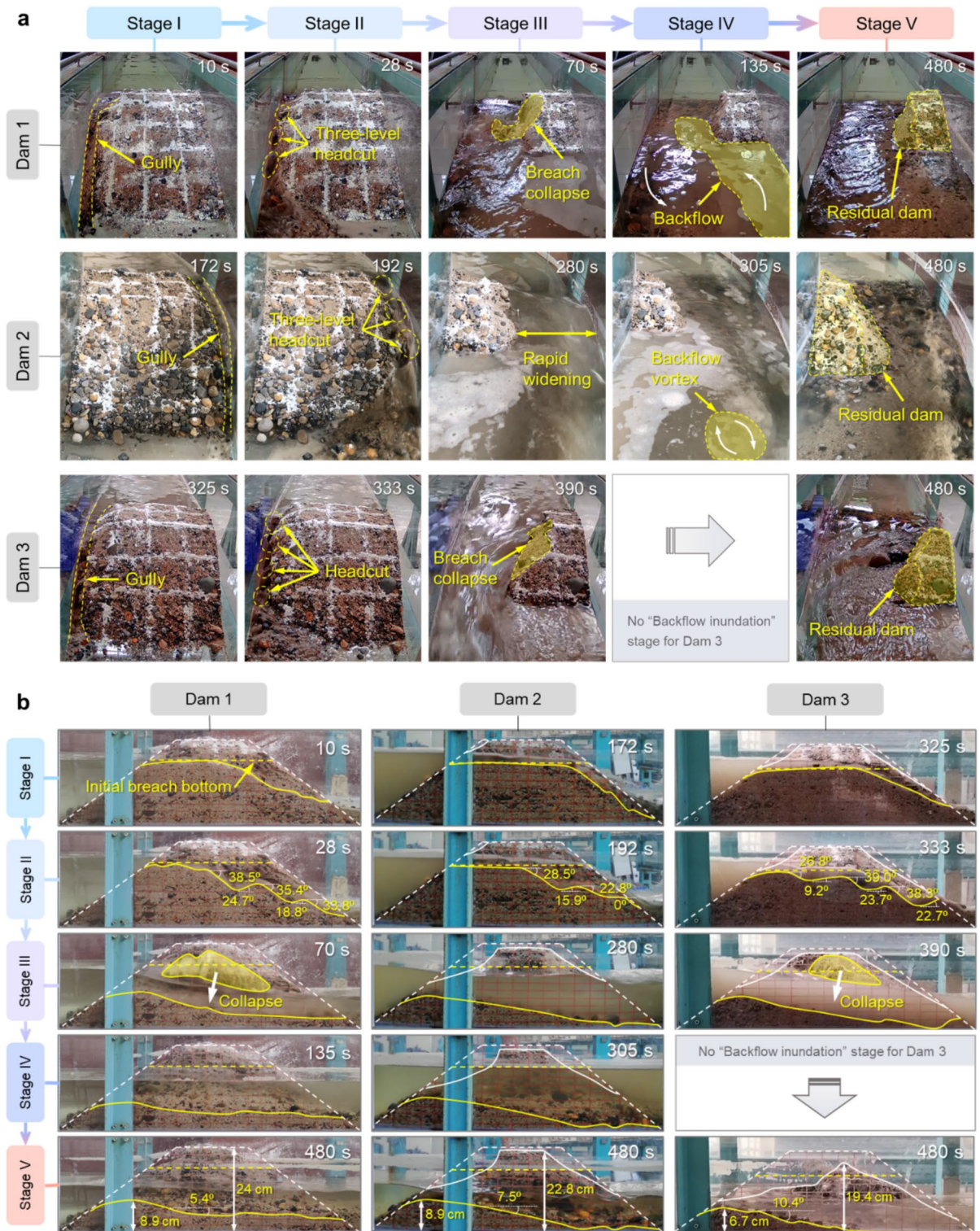
Fig. 5. Sequential stages of dam failure and geomorphological changes of the breach for the three cascade dams: (**a**) Photographic sequence showing the failure process of Dam 1, Dam 2, and Dam 3 across five stages: Stage I (Diversion Erosion), Stage II (Headward Erosion), Stage III (Breach Development), Stage IV (Backflow Inundation, when applicable), and Stage V (Water Level Decrease). The timeline for each stage is provided in seconds. Yellow arrows indicate the progression of key processes, such as gully formation, headcut collapse, and backflow. Note that Dam 3 does not exhibit a "backflow inundation" stage due to hydrodynamic constraints; (**b**) Cross-sectional profiles of the breach bottom at different stages for all three dams. Initial breach configurations, breach widening, and residual profiles are marked with dashed and solid lines. Key measurements, including breach width, slope angles, and erosion depths, are labeled for each stage to illustrate geomorphological evolution. $t = 0$ indicates the moment when the water level in the reservoir of Dam 1 reaches the bottom of the breach.
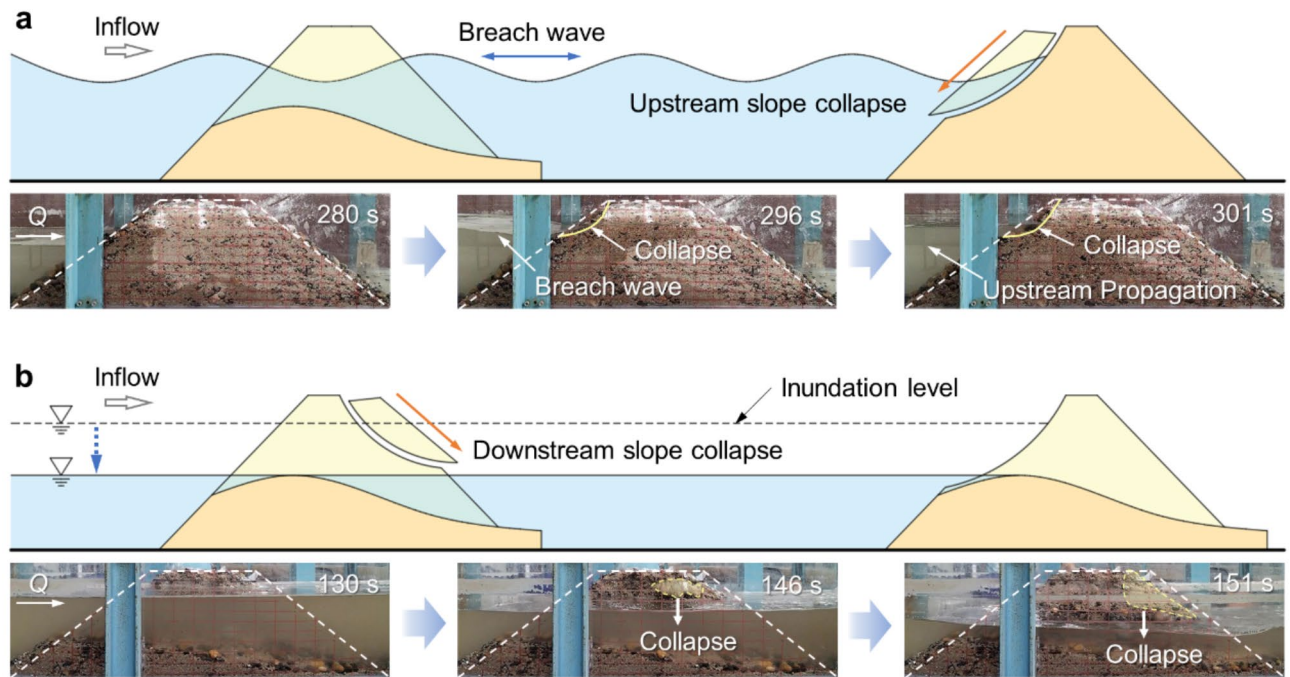
Fig. 6. Breaching forms after the peak breach flow: (**a**) Slope failure caused by the propagation of the breach wave (Dam 2 in Test 6); (**b**) Slope failure caused by the decrease in reservoir water level (Dam 2 in Test 6).

particle size differences exacerbate the heterogeneous initiation of the soil, promoting the formation of scour pits and triggering headcut erosion. Notably, landslide dam materials generally contain clay particles and exhibit wide-graded characteristics, thus the breaching process is often prominently characterized by headcut erosion.

When the breach flow increases rapidly in the early stages of dam breaching, the longitudinal expansion of the breach is mainly characterized by layer erosion. Layer erosion involves the gradual stripping of the dam material layer by layer and may also be accompanied by the instability and sliding of the upstream and downstream slopes, significantly reducing the thickness of the remaining dam body. For the breaching process of cascade landslide dams, the impact of layer erosion is particularly significant, as it not only accelerates the overall failure of the dam but also further complicates and makes the prediction of the breach more difficult through the sliding actions.

In this study, a U-shaped flume was employed, and it is well understood that the presence of bends can indeed alter the flow path and hydrodynamic characteristics. For instance, in curved sections, the centrifugal force causes water to concentrate along the outer bank, leading to an increase in flow velocity on the outer side and a corresponding decrease on the inner side. This phenomenon results in a deflection of the breach wave propagation direction and affects the steepness of the wavefront. Additionally, flow in the bend introduces more friction, turbulence, and energy dissipation, which may cause the breach wave to lose some energy compared to straight sections.

From the perspective of breach mechanisms, flow in the bend can induce asymmetric lateral erosion of the breach and localized hydrodynamic intensification. However, in this study, the influence of bend flow on the breach process was not the primary focus. As a result, the initial breach was positioned along the outer bank of the bend, minimizing the manifestation of asymmetric erosion and hydrodynamic intensification effects. Consequently, the breach mechanisms observed for the three dams showed certain similarities, consistent with the failure modes described earlier.

Breaching characteristics

Based on the results of the experiments conducted in this study, several representative parameters, such as breach outflow, breach dimensions, and reservoir water level evolution, were analyzed to understand the mechanism of overtopping failure in cascade landslide dams. This analysis also aims to distinguish the differences between the failure processes of cascade landslide dams and single dams. The evolution of breach outflow and reservoir water level for cascade landslide dams in Test 1 is shown in Fig. 7.

Based on the results from Test 1, where the overtopping failure of the cascade landslide dams was examined, Dam 1 was the first to experience overtopping failure due to the continuous inflow from upstream. The breach flow rate peaked at 13.3 L/s at 89.8 s. During this time, as the breach flow increased, the upstream reservoir water level began to drop. When the water level fell to 8.1 cm, Dam 1 entered Stage IV. The backflow from Dam 2 caused the water level to rise again, and the breach erosion halted after 125 s.

Sixteen seconds after Dam 1 began to discharge, the flow reached Dam 2. Due to the larger reservoir capacity of Dam 2 compared to Dam 1, the water level in Dam 2 rose more slowly with the same inflow rate. Dam 2 began to breach after 142 s, with the flow rate starting to increase after 51 s and reaching its peak of 12.5 L/s at 100 s.
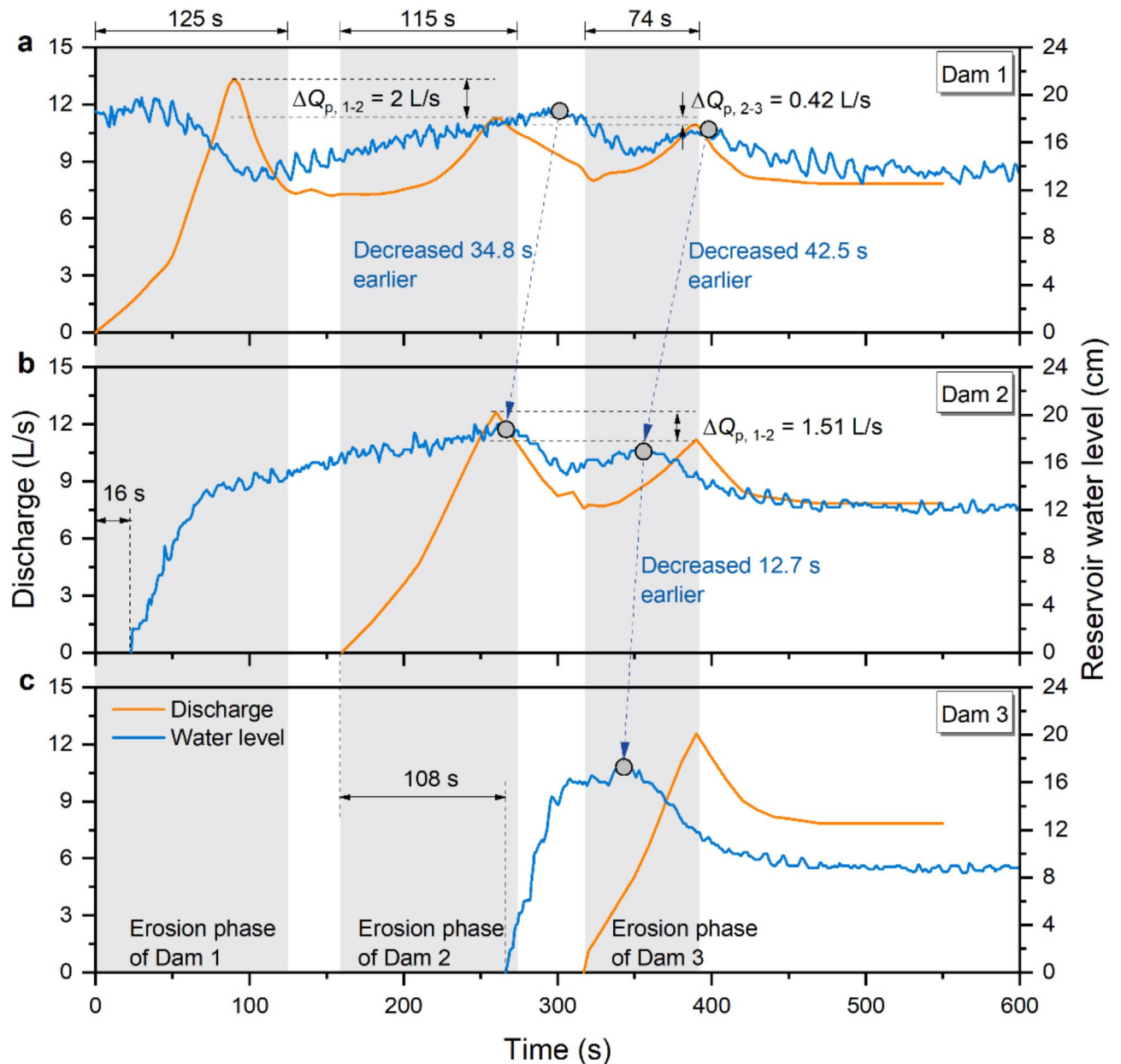
Fig. 7. Evolution of breach flow rate and reservoir water level in cascade landslide dams during Test 1: (**a**) Dam 1; (**b**) Dam 2; (**c**) Dam 3. The reservoir water level refers to the water level at the dam heel. $t = 0$ indicates the moment when the water level in the reservoir of Dam 1 reaches the bottom of the breach.

At the same time, the flow rate at Dam 1 also reached a peak, which was 2 L/s lower than its initial breach peak. After the peak, the reservoir water level in Dam 2 began to decrease first, followed by Dam 1 with a delay of 34.8 s. After 115 s, the erosion of Dam 2's breach stopped, but the breach flow and reservoir water level continued to decline, and Dam 2 entered Stage IV after 146 s.

When Dam 2 started discharging, the breach flow at the early stage of Dam 2's failure increased slowly. The flow reached Dam 3 after 108 s, and Dam 3 began storing water. Fifty-one seconds later, Dam 3 started to breach, with a rapid failure progression. The flow rate peaked at 12.4 L/s, 72 s after the breach initiation. Simultaneously, the flow rates at Dams 1 and 2 also peaked again, with Dam 1's flow rate decreasing by 0.42 L/s and Dam 2's by 1.15 L/s. The reservoir water levels in both upstream dams peaked before the flow rates, with significant time lags: Dam 2 lagged by 12.7 s and Dam 1 by 55.2 s.

Based on the analysis of the breach processes in these three cascade landslide dams, it can be observed that, overall, the breaching of cascade landslide dams tends to intensify the breach process of downstream dams, resulting in higher peak flow rates, earlier peak times, and shorter erosion durations. Specifically, the upstream dam experiences peak flow rates during both its own breach and the breach of the downstream dam, with the peak flow rate gradually decreasing. The extent of this decrease diminishes with increasing distance downstream.

The erosion duration (Stage I-III) for the downstream dams is significantly shorter than that for the upstream dam, indicating more intense erosion downstream. However, in the case of landslide dams located at a bend, if the initial breach is on the outer side of the bend, it can noticeably slow the increase in breach flow, prolong the breach duration, and make the overall breach process more gradual, which is beneficial for emergency response efforts.

The longitudinal down-cutting process of the breach and the variation in the slope of the breach bottom during the dam failure are crucial aspects in the study of dam breach mechanisms and modeling. In Fig. 8, the longitudinal profiles (a, c, e) show the stepwise retreat of the breach bottom over time at intervals of 10 s, highlighting key points such as the location of the scour pit and the apex of the breach bottom. The changes in bottom slope angles (b, d, f) are modeled using regression curves to illustrate the relationship between time and erosion dynamics. The equations and R^2 values quantify the temporal evolution of the slope, with critical phases such as toe scouring and stabilization annotated. Time $t = 0$ represents the moment when the water level in each reservoir reaches the bottom of the breach, marking the initiation of erosion processes.

As can be seen in Fig. 8, during the initial stage of outflow, the downstream end of the breach rapidly descends, forming an initial scour channel (Stage I). Simultaneously, the top of the breach progressively shifts
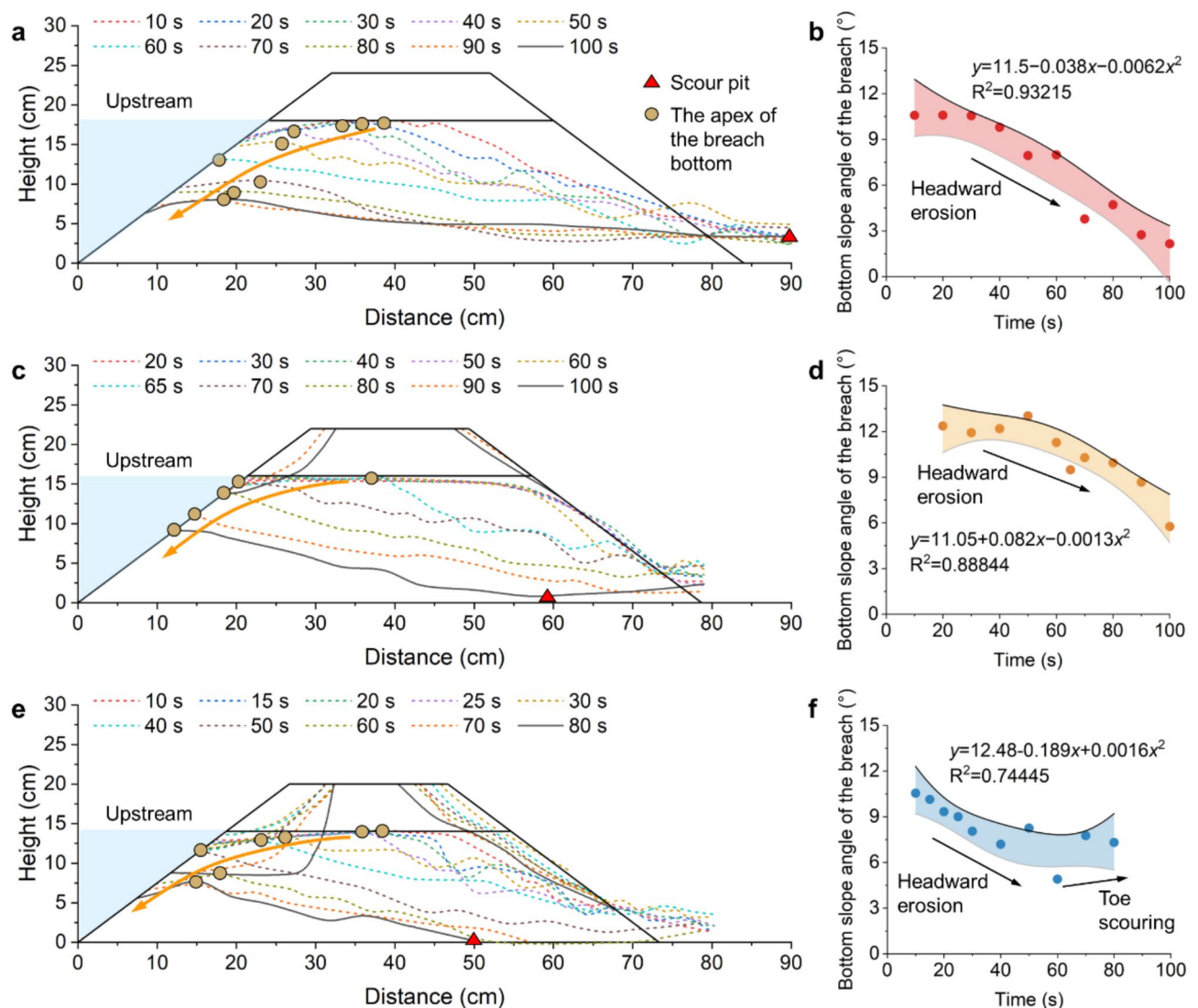

Fig. 8. Longitudinal geomorphic evolution and bottom slope angle dynamics of breaches in cascade landslide dams during Test 1: (**a**) Longitudinal geomorphic evolution of the breach in Dam 1 over time, illustrating the progression of headward erosion and scour pit formation; (**b**) Temporal evolution of the bottom slope angle in Dam 1, showing the reduction in slope angle due to headward erosion and stabilization trends; (**c**) Longitudinal geomorphic evolution of the breach in Dam 2, highlighting the migration of the breach apex and scour pit dynamics; (**d**) Temporal evolution of the bottom slope angle in Dam 2, with trends indicating erosion and toe scouring; (**e**) Longitudinal geomorphic evolution of the breach in Dam 3, emphasizing the headward erosion progression; (**f**) Temporal evolution of the bottom slope angle in Dam 3, showing trends of erosion and stabilization.

upstream (Stage II). For Dam 1, sediment accumulation occurs downstream of the breach, with a deposition thickness of 3.5 cm, resulting in a gradual decrease in the slope of the breach bottom during the breach process. For Dam 2, during Stage III, the intensity of breach erosion increases, reducing the sediment deposition height to 2.4 cm, and the scour pit shifts upstream to 58 cm. Consequently, the breach slope at the later stage of the dam failure is higher than that of Dam 1. In the case of Dam 3, the breach process is more intense, with rapid descent of the breach and no sediment accumulation downstream. The dam toe shifts further upstream to 50 cm, and an increase in the breach bottom slope is observed due to scour at the dam toe, which significantly differs from that of Dam 1.

Figure 9 illustrates the process of lateral expansion of the breach and the residual breach after the dam failure. It can be clearly observed that the duration of Stage I and Stage II for Dam 1 is relatively long, indicating that a significant amount of time after the initial outflow is dominated by vertical down-cutting of the breach. This includes the formation of a scour pit, the development of a steep slope, and upstream erosion. Once Stage III is reached, the lateral widening rate of the breach is 0.33 cm/s, lasting for 40 s, with two slope collapses occurring during the process. For Dam 2, the duration of Stage I and Stage II is shorter. However, because Dam 2 is located at a bend, the flow velocity on the outer side is greater than on the inner side, resulting in a lower lateral widening rate of 0.24 cm/s compared to Dam 1. Additionally, the lateral erosion duration is longer, lasting 65 s, with two slope collapses occurring throughout the process. As the downstream dam, Dam 3 experiences the most intense
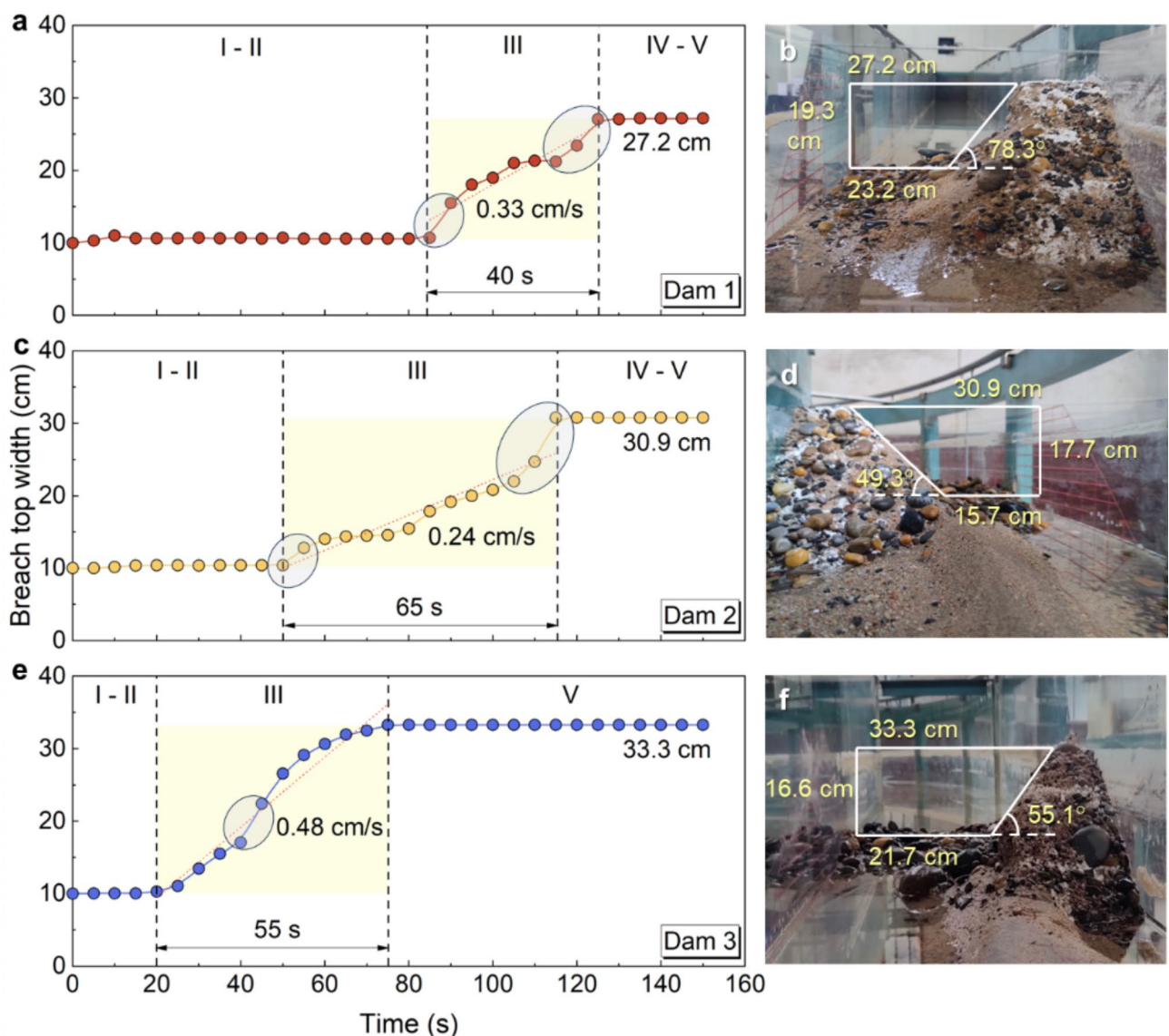
Fig. 9. Transverse geomorphic evolution of breach in cascade landslide dams in Test 1: (**a**) Evolution of the breach top width for Dam 1; (**b**) Residual dam of Dam 1; (**c**) Evolution of the breach top width for Dam 2; (**d**) Residual dam of Dam 2; (**e**) Evolution of the breach top width for Dam 3; (**f**) Residual dam of Dam 3. $t=0$ represents the moment when the water level in the reservoir of each dam reaches the bottom of the breach.

breaching process. After the initial outflow, it quickly enters Stage III, with a widening rate of 0.48 cm/s and a lateral erosion duration of 55 s, during which the slope collapses once.

Based on the above observations, it can be concluded that for cascade landslide dams, the upstream dam exhibits longer durations in Stage I and Stage II, with a lower breach expansion rate in Stage III due to a lower head at the breach. The continued scouring at the base of the breach led to multiple slope collapses. Conversely, the downstream dam experiences a more intense breaching process, with shorter durations in Stage I and Stage II, a faster breach expansion rate, and greater challenges in emergency management. As a result of the more intense erosion process, the residual breach size in the downstream dam is larger than that in the upstream dam.

Discussion
The influence of inflow
In general, the overall process of overtopping failure of the three cascade landslide dams, the stage division, and the mechanisms observed at each stage are similar in the first three tests conducted. Given this similarity, this section now focuses on a quantitative analysis of how different inflow rates impact the cascading failure of the model dams. The results of this analysis are illustrated in Fig. 10.

The impact of inflow rate on the dam breach process is significant and follows an obvious pattern. For breach flow, an increase in inflow rate markedly raises the peak breach flow, and this effect becomes more pronounced as the inflow increases. Additionally, as mentioned earlier, the failure of downstream dams can also increase the flow
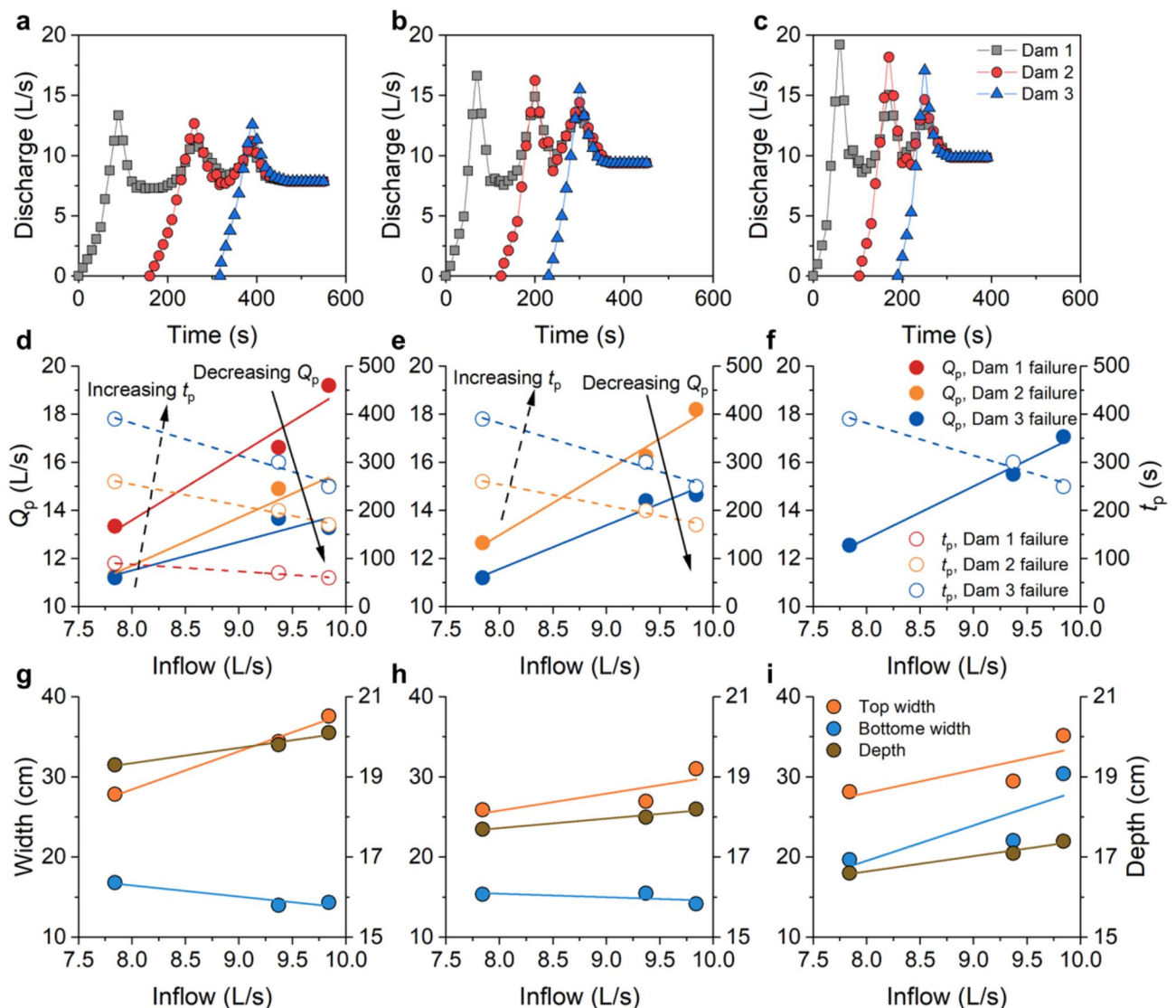
Fig. 10. Influence of inflow on the overtopping failure process of cascade landslide dams: (**a**) Breach flow in Test 1; (**b**) Breach flow in Test 2; (**c**) Breach flow in Test 3; (**d**) Characteristic values of breach flow for Dam 1; (**e**) Characteristic values of breach flow for Dam 2; (**f**) Characteristic values of breach flow for Dam 3; (**g**) Residual breach dimensions for Dam 1; (**h**) Residual breach dimensions for Dam 2; (**i**) Residual breach dimensions for Dam 3. Q_p represents the peak flow rate, and t_p represents the time to peak flow.

rate at the upstream dam section. Interestingly, however, the peak flow at the upstream dam due to downstream dam failure initially increases with rising inflow but then decreases. This suggests that once the inflow reaches a certain level, the influence of downstream dam failure on upstream dam flow weakens. Regarding the timing of peak flow, it is evident that as the inflow increases, the peak time shifts earlier. The influence of downstream dam failure on the upstream dam's peak timing also becomes more pronounced.

For the residual breach after dam failure, there is a clear positive correlation between inflow and breach depth. However, the experimental results reveal an interesting pattern concerning breach width. The top width of the breach consistently shows a positive correlation with inflow. In contrast, for bottom width, the upstream dams exhibit a positive correlation with inflow, while the downstream dams show a negative correlation. This phenomenon can be explained by the fact that at lower inflows, the head at the upstream dam's breach is smaller, leading to faster erosion at the bottom than at the top. Conversely, at higher inflows, the breach is more submerged, causing the top of the breach to expand more rapidly, resulting in a gentler side slope and a wider cross-section. Consequently, as inflow increases, the bottom width of the breach decreases. For the downstream dams, which have larger reservoir capacities and more intense breach processes, the breach development is more complete, leading to a positive correlation between breach width and inflow.

The influence of height of the middle dam

In the context of overtopping failure of a single landslide dam, there is a general consensus within the academic community on the influence of dam height on the breach process[18,19,47]. However, there is no agreed understanding in the current literature when it comes to cascade landslide dams, particularly the impact of the height of the middle dam on the failure of both upstream and downstream dams, as well as its own failure. Therefore, this study aims to investigate the influence of the middle dam height in cascade landslide dams on the breach process by comparing the results of Test 1 and Test 4. The focus of the analysis is on key parameters such as the breach flow process, flow characteristics, and residual breach dimensions, as illustrated in Fig. 11.

Based on the experimental results, the height of the middle dam in a cascade of landslide dams has some impact on the dam breach process, displaying certain patterns. Regarding the breach flow process, the peak flow rate and peak time of the upstream dam are not significantly affected by the height of the middle dam, as they are primarily influenced by the hydraulic conditions upstream and of the dam itself. However, since the downstream dam's failure is influenced by the middle dam's height, the peak flow time caused by the downstream dam's breach is delayed as the middle dam's height increases. For the middle dam itself, as the height increases, the peak breach flow rate also increases, and the peak time is further delayed, consistent with existing knowledge. As for the downstream dam, the increased height of the middle dam leads to a delay in the peak flow time but results in a slight reduction in the peak flow rate. The main reason for this is that the increased height of the middle dam extends its breach duration and delays the peak time, reducing the flood pressure downstream, which slightly lowers the peak flow rate of the downstream dam.

Regarding the residual breach dimensions after failure, the increased height of the middle dam increases the total flow through the river channel cross-section, leading to more extensive scouring of the dam and a corresponding extension of the scouring duration. Consequently, the breach develops more fully. For breach width, all three dams show a consistent trend of increasing width with the increase in the height of the middle dam. For breach depth, the downstream dam's depth increases with the height of the middle dam, while the upstream dam is not significantly affected.

The influence of step spacing

When a series of landslide dams form along a river channel, the spacing between these dams, known as step spacing, may vary. This section presents a comparative analysis of the results from Test 1, Test 5, and Test 6, focusing on the impact of step spacing on the overtopping failure process of cascade landslide dams, as illustrated in Fig. 12.

The influence of step spacing on the dam breach process does not follow a clear and consistent pattern. Regarding breach flow rate, the upstream dam's peak flow rate and peak time are minimally affected by increasing step spacing. However, for the middle dam, both peak flow rate and peak time increase with step spacing, while the downstream dam experiences a delay in peak flow time as the spacing increases, and the peak flow rate first decreases and then increases. As for the residual breach after dam failure, step spacing has a greater impact on the downstream dam compared to the upstream dam. The residual breach width of the upstream and middle dams is not particularly sensitive to step spacing. In contrast, for the downstream dam, breach width decreases initially and then increases with increased spacing. Breach depth is less affected by step spacing, exhibiting a rough, slight positive correlation.

The relatively weak consistency (monotonicity) observed in the effect of step spacing, particularly for the downstream dam, can be explained as follows: Larger step spacing increases the downstream dam's reservoir capacity, which in turn leads to a more intense breach process, such as higher peak flow rates. However, increased step spacing also means that the downstream dam is located farther from the upstream dam, thereby weakening the influence of the upstream dam's breach on the downstream dam. These two opposing effects tend to cancel each other out. Therefore, the impact of step spacing on the downstream dam breach process depends on which of these effects becomes dominant.

Correlation analysis of breach parameters

The failure characteristics obtained from six sets of experiments under varying input conditions are presented in Appendix A. Based on the data listed in this appendix, the correlation between the input parameters and output data of this study can be computed, as shown in Fig. 13.
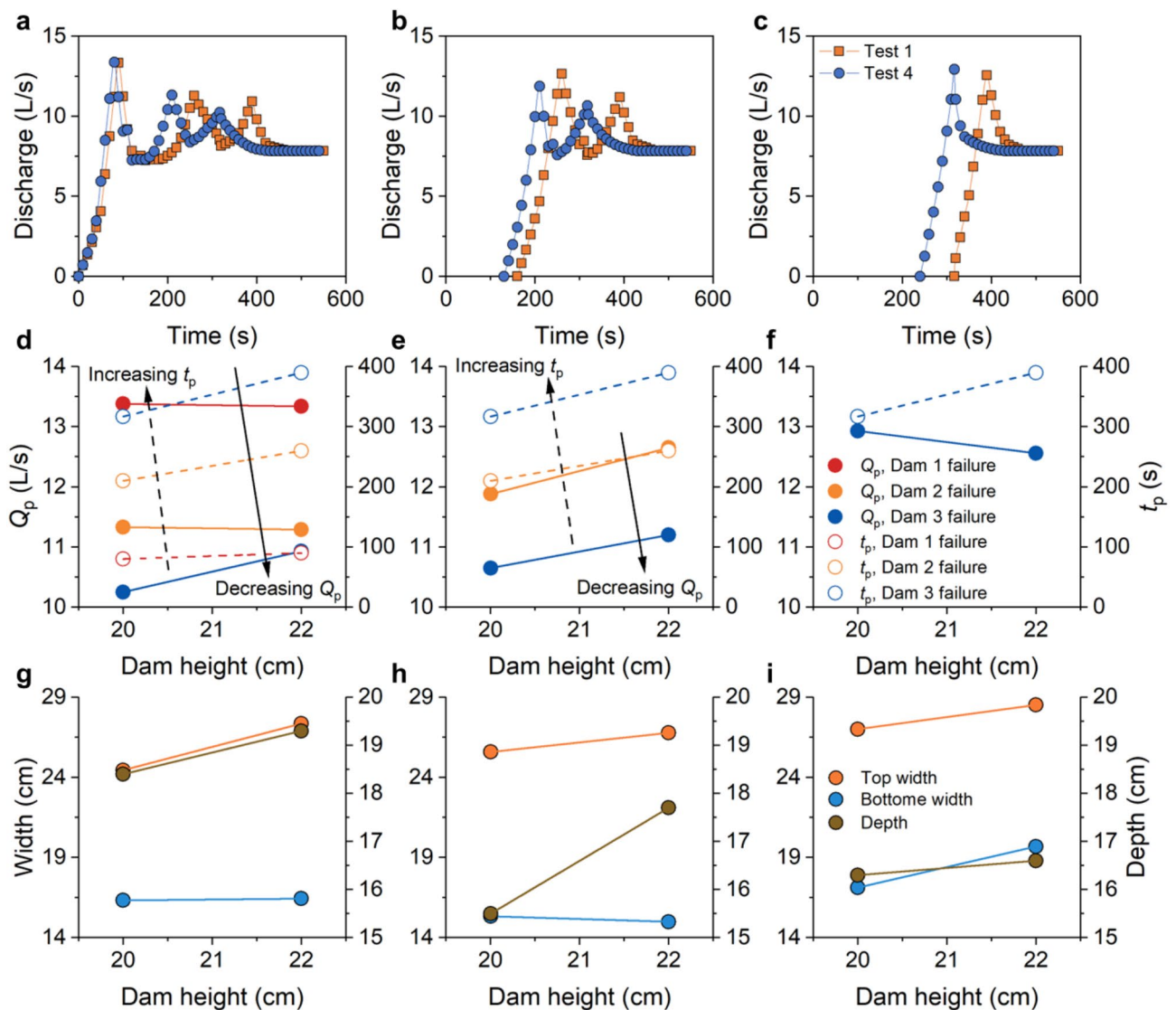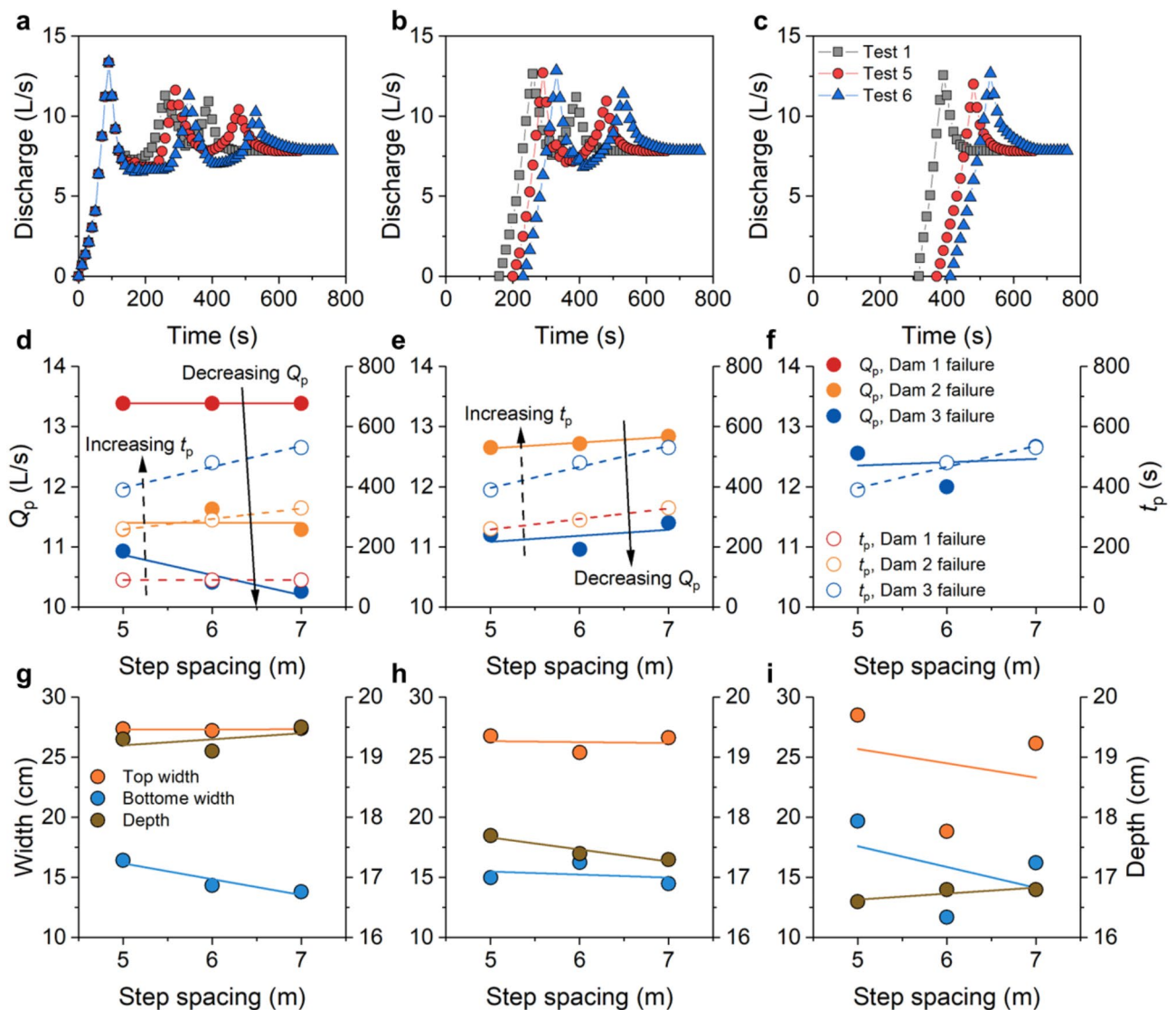
Fig. 11. Influence of middle dam height on the overtopping failure process of cascade landslide dams: (**a**) Breach flow of Dam 1; (**b**) Breach flow of Dam 2; (**c**) Breach flow of Dam 3; (**d**) Characteristic values of breach flow for Dam 1; (**e**) Characteristic values of breach flow for Dam 2; (**f**) Characteristic values of breach flow for Dam 3; (**g**) Residual breach dimensions for Dam 1; (**h**) Residual breach dimensions for Dam 2; (**i**) Residual breach dimensions for Dam 3. Q_p represents the peak flow rate, and t_p represents the time to peak flow.

Based on the correlation between several key parameters investigated in this study and the breach characteristics, it is evident that the parameters unique to cascade landslide dams have a significant and non-negligible impact on breach outcomes. This also highlights the distinct differences between overtopping failures of cascade landslide dams and single landslide dams. Regarding inflow rate, there is a clear positive correlation between inflow rate and peak breach flow rate. An increase in inflow rate leads to a rise in peak flow rate, as well as an increase in the residual breach width at the top, and likely also increases the width and depth at the base. Additionally, a higher inflow rate tends to advance the timing of peak flow rate, thus shortening the downstream evacuation time.

For the parameters unique to cascade landslide dams, the height of the intermediate dam has a relatively minor effect on the breach process. Increasing step spacing results in a reduction of peak flow rate and a delay in peak timing, with this effect becoming more pronounced as step spacing increases. The step index significantly affects the timing of peak flow rate, showing a certain positive correlation with peak breach flow rate. Although the peak flow rate for Dam1 is generally higher than that for Dam3, this is attributed to Dam1 having a greater dam height, which increases the peak flow rate. Excluding the effect of dam height on peak flow rate, the cascade landslide dam breaches show an increasing peak flow rate from upstream to downstream, reflecting an amplification effect of peak flow rate during the breach process. Additionally, peak timing is advanced, and residual breach depth increases, indicating that the breach severity increases from upstream to downstream. The affected step index indicates that as the distance downstream increases, the peak flow rate of the upstream dams
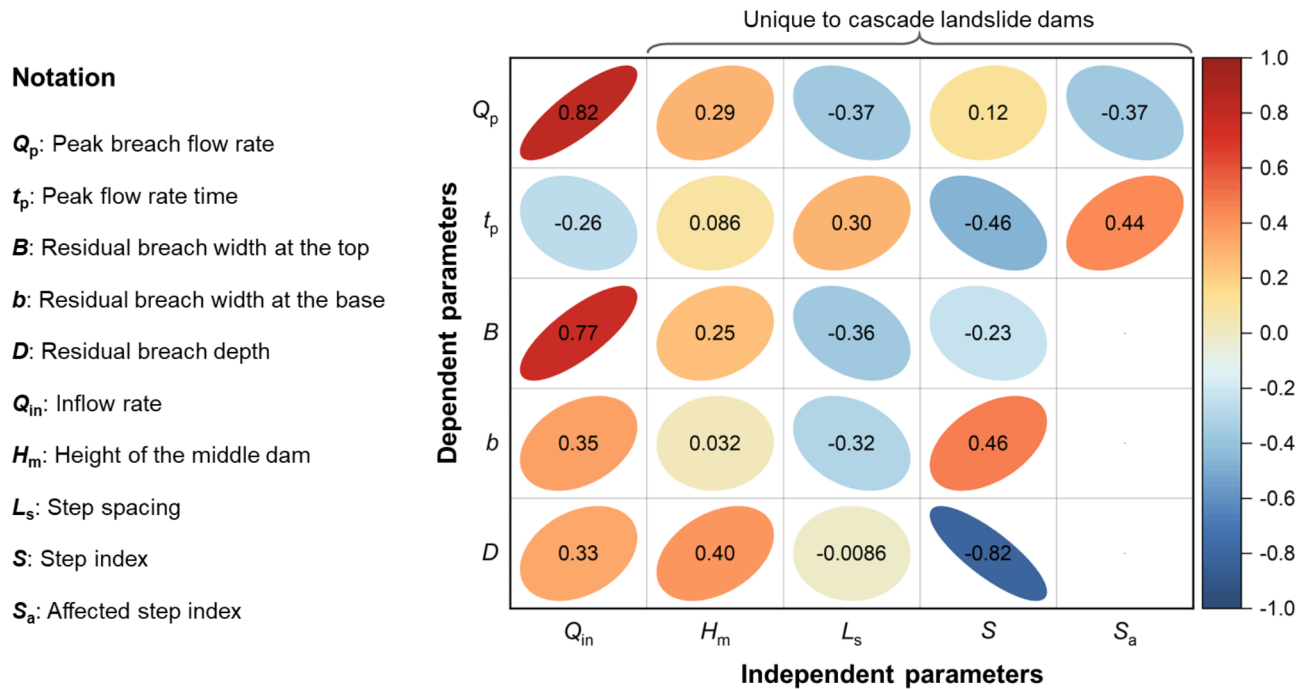
Fig. 12. Influence of step spacing on the overtopping failure process of cascade landslide dams: (**a**) Breach flow of Dam 1; (**b**) Breach flow of Dam 2; (**c**) Breach flow of Dam 3; (**d**) Characteristic values of breach flow for Dam 1; (**e**) Characteristic values of breach flow for Dam 2; (**f**) Characteristic values of breach flow for Dam 3; (**g**) Residual breach dimensions for Dam 1; (**h**) Residual breach dimensions for Dam 2; (**i**) Residual breach dimensions for Dam 3. Q_p represents the peak flow rate, and t_p represents the time to peak flow.

decreases and peak timing is delayed, meaning that the further downstream, the lesser the impact on upstream dams.

Insights for cascade landslide dam breach models

Landslide dam breaches can trigger catastrophic dam-break floods, with the scale and temporal evolution of these floods being influenced by dam erosion, which, in turn, affects the erosion process itself[30,48,49]. Based on the findings of this study, cascade landslide dams exhibit an amplification effect on dam-break floods, and the potential disastrous consequences of this effect warrant greater attention. Therefore, accurately calculating the overtopping erosion process of cascade landslide dams and accurately predicting the flood hydrograph during dam failure are critical.

Following a dam breach, dam-break waves may form downstream. Although these waves might have a limited impact on a single dam breach, they can significantly influence the breach profiles of cascade landslide dams. As shown in Fig. 6; Table 5, conceptual diagrams from this study illustrate how erosion shapes these profiles. Specifically, these waves can cause slope collapse during the water retention phase of downstream dams, which reduces dam thickness and weakens the dam's water-retention capacity. Notably, they also contribute to the reduction of breach length. Furthermore, fluctuations in reservoir water level due to dam-break waves may result in intermittent erosion of the breach during Stage I, extending the duration of Stage I and delaying the peak flow time, which could lead to conservative estimates in calculations.

Notation

Q_p: Peak breach flow rate

t_p: Peak flow rate time

B: Residual breach width at the top

b: Residual breach width at the base

D: Residual breach depth

Q_{in}: Inflow rate

H_m: Height of the middle dam

L_s: Step spacing

S: Step index

S_a: Affected step index

Fig. 13. Correlation analysis of dam breach parameters.

There are differences in the bottom slope erosion morphology and sedimentation patterns of the breach at different step indices. For instance, the breach bottom slope of upstream dams tends to flatten out at the end of the dam breach process, with sediment accumulation occurring at the dam toe, i.e., the downstream channel. In contrast, downstream dams experience more intense erosion, with little to no downstream sedimentation, resulting in a steeper breach bottom slope. Furthermore, intermittent collapse during lateral breach expansion is more prevalent in upstream dams. In downstream dams, due to more intense erosion and higher water head at the breach, the breach expansion is dominated by continuous erosion. Therefore, in modeling cascade landslide dam failures, it is important to establish reasonable criteria for breach slope collapse.

Most importantly, there is currently no dedicated mathematical model for cascade landslide dam breaches. Typically, dam breach models and flood routing models are used separately to compute different stages, but this approach cannot adequately account for the influence of riverbed morphological evolution on water flow throughout the river channel, nor can it properly consider the coupling effects between upstream and downstream dams. Since cascade landslide dam failures are not merely the propagation of single-dam breach floods, and there are differences in the failure mechanisms, our experimental results further reveal the fundamental correlation between the step index and breach morphology evolution, as well as erosion mechanisms in cascade landslide dam failures. Current dam breach models cannot fully capture these mechanisms. Taking these issues into account is expected to enhance the predictive capabilities of cascade landslide dam failure models and contribute to the future development of three-dimensional landslide dam erosion models.
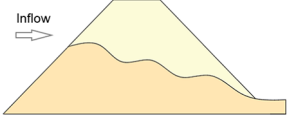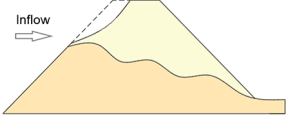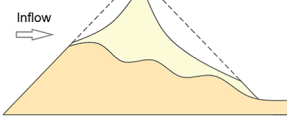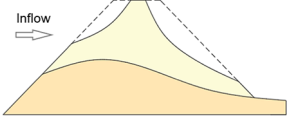
Comparison with existing studies

The cascading failure of landslide dams presents unique challenges compared to the failure of single dams. While several studies have focused on single dam failures in straight channels, research on cascading dam failures under realistic conditions, such as curved river sections, remains limited. This study aims to bridge these gaps by experimentally investigating cascading failures in a U-shaped flume, which mimics natural river conditions more closely. In this section, the novelty and contributions of the present study are compared with existing state-of-the-art approaches.

As summarized in Table 6, existing studies have significantly advanced the understanding of landslide dam failures, particularly in the context of single dam breaches. Building on this foundation, the present study introduces a more realistic representation of river bends and cascading systems, providing novel insights into asymmetric hydrodynamic behaviors and erosion dynamics. Moreover, by systematically analyzing flood wave amplification and attenuation between dams, this study helps bridge the knowledge gap in understanding cascading failures. This focus on cascading interactions distinguishes the present work from existing studies, which primarily emphasize peak discharge predictions or sediment transport processes in single dam scenarios. The findings of this study offer actionable recommendations for flood mitigation strategies, dam design, and emergency response planning in cascading systems, addressing challenges that have been less explored in previous research. As such, this study serves both as a foundation for future research and as a reference for improving disaster risk management.

Aspect	This study	Complementary insights from existing studies	Contribution of this study
Experimental setup	Large-scale U-shaped flume with bends and cascading dams	Existing studies often use straight flume setups or numerical models, offering controlled conditions for single dam failures[22,45,50]	Introduces a U-shaped flume to simulate river bends and cascading systems, enhancing realism in experimental studies
Focus	Cascading landslide dam failures, emphasizing flood amplification and attenuation dynamics	Significant progress has been made in understanding single dam failures and their downstream impacts[22,45,51]	Expands upon prior research by systematically analyzing cascading dam interactions and their hydrodynamic impacts
Key contributions	Systematic analysis of flood wave dynamics, breach evolution, and amplification/attenuation mechanisms	Existing works highlight peak discharge and erosion in single dam failures, providing foundational knowledge[18,36]	Builds on this foundation to explore cascading systems, addressing complex wave interactions and breach progression
Hydrodynamic insights	Detailed analysis of flow asymmetry, erosion dynamics, and breach evolution in bends and cascades	Insights into generalized hydrodynamics and erosion from previous studies have provided key theoretical frameworks[18,52]	Advances this understanding by examining asymmetric erosion and localized energy dissipation in realistic settings
Limitations	Laboratory-scale experiments without direct field validation	Field-based studies, such as Tangjiashan cases, provide critical real-world validation for dam failures[45,53]	Provides a controlled experimental basis to guide future field studies and numerical simulations
Applications	Practical implications for flood risk mitigation and cascading dam design	Applications have focused on site-specific scenarios[41,54]	Offers actionable insights for cascading systems, including design and emergency planning recommendations

Table 6. Key comparisons between the proposed study and existing research on cascading landslide dam failures.

Test conditions	Q_p (L/s)	t_p (s)	Erosion characteristics	Failure patterns
Dam 1 in Test 1	13.34	90.2	1. Headcut erosion 2. Headward erosion	
Dam 1 in Test 4	13.38	82.1		
Dam 3 in Test 4	12.93	318.9		
Dam 1 in Test 5	13.39	90.7		
Dam 1 in Test 6	13.39	91.4		
Dam 2 in Test 6	12.84	330.2		
Dam 1 in Test 2	16.62	72.3	1. Headcut erosion 2. Headward erosion 3. Upstream slope collapse	
Dam 2 in Test 2	16.25	202.7		
Dam 3 in Test 6	12.67	532.1		
Dam 2 in Test 1	12.65	261.3	1. Headcut erosion 2. Headward erosion 3. Upstream slope collapse 4. Downstream slope collapse	
Dam 3 in Test 1	12.56	392.5		
Dam 3 in Test 2	15.51	304.2		
Test 4, Dam 2	11.88	210.5		
Test 5, Dam 2	12.72	290.1		
Test 5, Dam 3	12	481.1		
Test 3, Dam 1	19.2	61.8	1. Layer erosion 2. Upstream slope collapse 3. Downstream slope collapse	
Test 3, Dam 2	18.19	171.6		
Test 3, Dam 3	17.07	253.5		

Table 5. Failure patterns and breach process for all test conditions. In the table, Q_p denotes the peak flow rate at the breach, and t_p denotes the time at which the peak flow rate occurs.

Conclusions

This study investigated the breaching process of cascade landslide dams under overtopping conditions through six sets of experiments. The key hydraulic parameters during the breaching process and the dynamic evolution of breach morphology were thoroughly analyzed. We identified that the breaching process of cascade landslide dams can be divided into three main stages: the rise of the phreatic line, overtopping breach, and submersion of the residual dam. The rate of phreatic line rise is primarily influenced by inflow, while its shape and inclination are largely affected by the permeability coefficient and its spatial distribution within the dam body, with minimal correlation to the dam's geometric characteristics.

Focusing on the overtopping breach phase, we categorized it into five distinct stages: initial gully formation characterized by a rapid decline in the slope of the breach bed; development and migration of the breach pit, during which the breach bed slope remains relatively constant; rapid breach expansion with a significantly higher horizontal expansion rate than vertical; backflow submersion potentially causing instability and collapse of downstream dam slopes; and water level recession, which poses a risk of collapse for the upstream dam slope. Additionally, four main failure patterns were identified: uneven surface erosion stress leading to gully formation and headcut erosion under low flow conditions; layer erosion during high flow rates; slope failures

due to significant fluctuations in river water levels between cascades; and collapses in dams with loose structures and high moisture content.

As the cascade sequence progresses from upstream to downstream, the peak flow rate at the breach increases with each successive stage, demonstrating a flood wave amplification effect between the cascades. This finding is consistent with the conclusions of previous studies conducted by some researchers using both experimental[18,50] and numerical[51,55] methods. Moreover, the timing of the peak flow also occurs earlier with each cascade, which significantly increases the challenges associated with emergency response and rescue efforts compared to single landslide dam breach scenarios. This impact diminishes as the distance between cascades increases. Given these differences, it is essential to develop specialized mathematical models for cascade landslide dam failures to enhance the accuracy of flood predictions and improve response strategies.

It is important to emphasize a critical point: although this study observed the occurrence of peak flow amplification during the cascading failure of landslide dams, which is consistent with current research findings, further investigation is required to determine whether this phenomenon is universally applicable to cascading dam failure scenarios. The propagation of breach waves between different cascade dams is influenced by multiple factors, such as the characteristics of upstream and downstream breach floods, the spatial distribution of landslide dams, and the storage capacity of downstream landslide-dammed lakes[55]. Specifically, when the upstream dam has a large water volume and experiences a rapid breach, resulting in highly concentrated flood energy, cascading failures are more likely to exhibit peak flow amplification. In contrast, when the flood peak from the upstream breach is relatively small, or the downstream landslide-dammed lake has low water levels, a stable dam structure, and sufficient storage capacity, downstream landslide dams may exhibit a peak attenuation effect. Therefore, further investigations are necessary to understand whether peak flow amplification or attenuation dominates in the cascading failure process of landslide dams. Such research would provide valuable insights into the underlying mechanisms of cascading failures and their implications for risk assessment and mitigation.

This study introduces a new perspective on the relationship between the erosion process of cascade landslide dams and their unique characterization parameters, and provides insights into the development of mathematical models for cascade landslide dam failures, thereby offering more accurate physical-based flood predictions. However, due to the multi-stage structure, cascade landslide dams face more complex issues related to erosion stress distribution, flow redistribution, and energy transfer during breaching. Future work will benefit from large-scale model experiments that account for these factors and their impact on the breaching process of cascade landslide dams.

Data availability
Data is provided within the manuscript or supplementary information files.

References
1. Yang, Q., Guan, M., Peng, Y. & Chen, H. Numerical investigation of flash flood dynamics due to cascading failures of natural landslide dams. *Eng. Geol.* **276**, 105765 (2020).
2. Zhou, G. G. D. et al. A preliminary study of the failure mechanisms of cascading landslide dams. *Int. J. Sediment. Res.* **30**, 223–234 (2015).
3. Zhu, X., Cui, P., Chen, H., Tang, J. & Zou, Q. Effects of cascade failure of Dammed lakes on the evolution of rivers in Wenchuan Earthquake Region. *J. Sichuan Univ. (Engineering Sci. Edition).* **44**, 64–69 (2012). (**in Chinese**).
4. Liu, N. et al. Draining the Tangjiashan Barrier Lake. *J. Hydraul Eng.* **136**, 914–923 (2010).
5. Yin, Y., Wang, F. & Sun, P. Landslide hazards triggered by the 2008 Wenchuan Earthquake, Sichuan, China. *Landslides* **6**, 139–152 (2009).
6. Chen, Z., Zhang, Q., Chen, S., Wang, L. & Zhou, X. Evaluation of Barrier Lake Breach floods: Insights from recent Case studies in China. *WIREs Water.* **7**, e1408 (2020).
7. Xu, Q., Fan, X., Huang, R. & Westen, C. V. Landslide dams triggered by the Wenchuan Earthquake, Sichuan Province, South West China. *Bull. Eng. Geol. Environ.* **68**, 373–386 (2009).
8. Cui, P., Zhu, Y., Han, Y., Chen, X. & Zhuang, J. The 12 May Wenchuan Earthquake-Induced Landslide Lakes: Distribution and preliminary risk evaluation. *Landslides* **6**, 209–223 (2009).
9. Liu, N., Yang, Q. G. & Chen, Z. Y. *Risk Management of Landslide Dams* (Yangtze River, 2016). (**in Chinese**).
10. Zhong, Q., Chen, S. & Shan, Y. Prediction of the overtopping-induced breach process of the landslide dam. *Eng. Geol.* **274**, 105709 (2020).
11. Wu, S. et al. Study on catastrophic landslides triggered by 2008 great Wenchuan earthquake, Sichuan, China. *J. Eng. Geol.* **18**, 145–159 (2010). (**in Chinese**).
12. Costa, J. E. & Schuster, R. L. The formation and failure of natural dams. *Geol. Soc. Am. Bull.* **100**, 1054–1068 (1988).
13. Peng, M. & Zhang, L. M. Breaching parameters of landslide dams. *Landslides* **9**, 13–31 (2012).
14. Shen, D., Shi, Z., Peng, M., Zhang, L. & Jiang, M. Longevity analysis of landslide dams. *Landslides* **17**, 1797–1821 (2020).
15. Liu, W. et al. Outburst floods in China: A review. *Earth-Sci. Rev.* **197**, 102895 (2019).
16. Fan, X. et al. Spatial distribution of landslide dams triggered by the 2008 Wenchuan Earthquake. In: (eds Margottini, C., Canuti, P. & Sassa, K.) *Landslide Science and Practice: Volume 5: Complex Environment* 279–285. (Springer, 2013).
17. Shi, Z. M. et al. Cascading breaching of the Tangjiashan landslide dam and two smaller downstream landslide dams. *Eng. Geol.* **193**, 445–458 (2015).
18. Cao, Z., Yue, Z. & Pender, G. Landslide dam failure and flood hydraulics. Part I: Experimental investigation. *Nat. Hazards.* **59**, 1003–1019 (2011).
19. YANG, F., LIU, Z. H. O. U. X., CAO, X., HUANG, E. R. & S. Experimental study of Breach growth processes in sand dams of quake lakes. *J. Earthq. Tsunami.* **05**, 445–459 (2012).
20. Zhao, T., Chen, S., Fu, C. & Zhong, Q. Influence of diversion channel section type on landslide dam draining effect. *Environ. Earth Sci.* **77**, 1–9 (2018).
21. Zhao, T., Chen, S., Fu, C. & Zhong, Q. Centrifugal model test on the failure mechanism of barrier dam overtopping. *KSCE J. Civ. Eng.* **23**, 1548–1559 (2019).

22. Zhou, G. G. D., Li, S., Lu, X. & Tang, H. Large-scale landslide dam breach experiments: Overtopping and overtopping and seepage failures. *Eng. Geol.* **304**, 106680 (2022).

23. Wang, J. et al. Long-term and short-term disposal of landslide dams at Steep V-shaped valleys. *Landslides* **21**, 135–153 (2024).

24. Luo, H. et al. Experimental investigation on the formation and failure of landslide dams considering the landslide mobility and river flow. *Eng. Geol.* 107873 (2024).

25. Lee, M., Park, G., Park, C. & Kim, C. Improvement of grid independence test for computational fluid dynamics model of building based on grid resolution. *Adv. Civ. Eng.* 1–11 (2020). (2020).

26. Li, Y., Chen, A., Wen, L., Bu, P. & Li, K. Numerical simulation of non-cohesive homogeneous dam breaching due to overtopping considering the Seepage effect. *Eur. J. Environ. Civ. Eng.* **26**, 1993–2007 (2022).

27. Lai, Z., Zhao, J., Zhao, S. & Huang, L. Signed distance field enhanced fully resolved CFD-DEM for simulation of granular flows involving multiphase fluids and irregularly shaped particles. *Comput. Meth Appl. Mech. Eng.* **414**, 116195 (2023).

28. Zhou, M. et al. Two-phase modelling of erosion and deposition process during overtopping failure of landslide dams using GPU-accelerated ED-SPH. *Comput. Geotech.* **166**, 105944 (2024).

29. Zhou, G. G. D. et al. Experimental investigation on the longitudinal evolution of landslide dam breaching and outburst floods. *Geomorphology* **334**, 29–43 (2019).

30. Zhou, G. G. D., Lu, X., Xie, Y., Cui, K. F. E. & Tang, H. Mechanisms of the non-uniform breach morphology evolution of landslide dams composed of unconsolidated sediments during overtopping failure. *J. Geophys. Res. Earth Surf.* 127, eJF006664 (2022).

31. Zhou, Y. et al. Experimental study on morphological characteristics of landslide dams in different shaped valleys. *Geomorphology* **400**, 108081 (2022).

32. Zhu, X. et al. Experimental study on the longitudinal evolution of the overtopping breaching of noncohesive landslide dams. *Eng. Geol.* **288**, 106137 (2021).

33. Zhang, J., Yang, X., Fan, G., Li, H. & Zhou, J. Physical and numerical modeling of a landslide dam breach and flood routing process. *J. Hydrol.* **628**, 130552 (2024).

34. Muslim, H. S. M., Khan, S. A., Hussain, S., Jamal, A. & Qasim, H. S. A. A knowledge-based image enhancement and denoising approach. *Comput. Math. Organ. Theory* **25**, 108–121 (2019).

35. Mahmood, A., Khan, S. A., Hussain, S. & Almaghayreh, E. M. An adaptive image contrast enhancement technique for low-contrast images. *IEEE Access.* **7**, 161584–161593 (2019).

36. Cao, Z., Yue, Z. & Pender, G. Flood hydraulics due to cascade landslide damfailure. *J. Flood Risk Manag.* **4**, 104–114 (2011).

37. Niu, Z., Xu, W., Li, N., Xue, Y. & Chen, H. Experimental investigation of the failure of cascade landslide dams. *J. Hydrodyn.* **24**, 430–441 (2012).

38. Zhou, G. G. D. et al. Experimental study on the triggering mechanisms and Kinematic properties of large debris flows in Wenjia Gully. *Eng. Geol.* **194**, 52–61 (2015).

39. Zhang, Q., Hu, K., Liu, S. & Liu, W. Controls on the regional distribution of landslide dams and implications for Fluvial landform evolution in Bhutan and its surrounding area. *J. Mt. Sci.* **20**, 2107–2132 (2023).

40. Chen, Z. et al. Back analysis of the draining process of the Tangjiashan Barrier Lake. *J. Hydraul Eng.* **141** (2015).

41. Li, D., Nian, T., Tiong, R. L. K., Shen, Y. & Shao, Z. River blockage and impulse wave evolution of the baige landslide in October 2018: Insights from coupled DEM-CFD analyses. *Eng. Geol.* **321**, 107169 (2023).

42. Shi, Z., Zhang, G., Peng, M., Zhong, Q. & Cai, S. Experimental investigation on the breaching mechanisms of landslide dams with heterogeneous structures. *Adv. Eng. Sci.* **55**, 129–140 (2023). (**in Chinese**).

43. Liang, J. Fluvial process influenced by earthquake lakes and restoration of mountain rivers. *J. Sichuan Univ. (Engineering Sci. Edition)*. **41**, 13–17 (2009). (**in Chinese**).

44. Shan, Y., Chen, S., Zhong, Q. & Mei, S. A rapid prediction model for peak breach flow of landslide dams considering the grain composition of deposits. *J. Basic. Sci. Eng.* **31**, 584–598 (2023). (**in Chinese**).

45. Chen, S. et al. Emergency response and back analysis of the failures of earthquake triggered cascade landslide dams on the Mianyuan River, China. *Nat. Hazards Rev.* **19**, 5018005 (2018).

46. Zhao, T., Chen, S., Fu, C. & Zhong, Q. Centrifugal model tests and numerical simulations for Barrier Dam Break due to overtopping. *J. Mt. Sci.* **16**, 630–640 (2019).

47. Yan, J., Cao, Z., Liu, H. & Chen, L. Experimental study of Landslide Dam-Break Flood over Erodible Bed in open channels. *J. Hydrodyn. Ser. B* **21**, 124–130 (2009).

48. Cui, P. et al. Landslide-Dammed Lake at Tangjiashan, Sichuan Province, China (triggered by the Wenchuan Earthquake, May 12, 2008): Risk Assessment, Mitigation Strategy, and lessons learned. *Environ. Earth Sci.* **65**, 1055–1065 (2012).

49. Turzewski, M. D., Huntington, K. W. & LeVeque, R. J. The geomorphic impact of outburst floods: Integrating observations and numerical simulations of the 2000 Yigong Flood, Eastern Himalaya. *J. Geophys. Res. Earth Surf.* **124**, 1056–1079 (2019).

50. Hu, W. et al. Flow amplification from cascading landslide dam failures: Insights from flume experiments. *Eng. Geol.* **297**, 106483 (2022).

51. Huang, W. & Cao, Z. Numerical simulation of flood reinforcement due to cascade dam break. *Eng. J. Wuhan Univ.* **47**, 160–164 (2014). (**in Chinese**).

52. Vinuesa, R., Brunton, S. L. & McKeon, B. J. The transformative potential of machine learning for experiments in fluid mechanics. *Nat. Rev. Phys.* (2023).

53. Cai, Y. J. et al. Breaches of the Baige Barrier Lake: Emergency response and dam Breach Flood. *Sci. China Technol. Sci.* **63**, 1164–1176 (2020).

54. Fan, X. et al. The formation and impact of landslide dams—State of the art. *Earth-Sci. Rev.* **203**, 103116 (2020).

55. Zhong, Q. et al. Numerical investigation of hydro-morphodynamic characteristics of a cascading failure of landslide dams. *J. Mt. Sci.* **21**, 1868–1885 (2024).

Acknowledgements

Author contributions
T. Zhao, and C. Fu planned the campaign; T. Zhao, W. Wu, C. Fu and H. Li conducted model tests; T. Zhao and C. Fu analyzed the data; T. Zhao and C. Fu wrote the manuscript draft; W. Wu and D. Huo reviewed and edited the manuscript.

Declarations

Competing interests
The authors declare no competing interests.

Additional information
Supplementary Information The online version contains supplementary material available at https://doi.org/10.1038/s41598-025-89618-5.

Correspondence and requests for materials should be addressed to C.F. or T.Z.

Reprints and permissions information is available at www.nature.com/reprints.

Publisher's note Springer Nature remains neutral with regard to jurisdictional claims in published maps and institutional affiliations.